Naval Research Laboratory

Washington, DC 20375-5320

NRL/MR/6180--07-9095

Comparison of Fire and Smoke Simulator (FSSIM) Predictions with Hydraulic Fluid Spray Fire Test Data

JOHN B. HOOVER
FREDERICK W. WILLIAMS

Navy Technology Center for Safety and Survivability
Chemistry Division

December 10, 2007

REPORT DOCUMENTATION PAGE

Form Approved
OMB No. 0704-0188

1. REPORT DATE *(DD-MM-YYYY)*	**2. REPORT TYPE**	**3. DATES COVERED** *(From - To)*
10-12-2007	Final Report	1-10-2006 – 30-9-2007

4. TITLE AND SUBTITLE

Comparison of Fire and Smoke Simulator (FSSIM) Predictions with Hydraulic Fluid Spray Fire Test Data

5a. CONTRACT NUMBER

5b. GRANT NUMBER

5c. PROGRAM ELEMENT NUMBER

6. AUTHOR(S)

John B. Hoover and Frederick W. Williams

5d. PROJECT NUMBER

5e. TASK NUMBER

5f. WORK UNIT NUMBER

7. PERFORMING ORGANIZATION NAME(S) AND ADDRESS(ES)

Naval Research Laboratory
4555 Overlook Avenue, SW
Washington, DC 20375-5320

8. PERFORMING ORGANIZATION REPORT NUMBER

NRL/MR/6180--07-9095

9. SPONSORING / MONITORING AGENCY NAME(S) AND ADDRESS(ES)

Office of Secretary of Defense
Joint Live Fire Test & Evaluation
The Pentagon
Washington, DC 20301-3090

10. SPONSOR / MONITOR'S ACRONYM(S)

11. SPONSOR / MONITOR'S REPORT NUMBER(S)

12. DISTRIBUTION / AVAILABILITY STATEMENT

Approved for public release; distribution is unlimited.

13. SUPPLEMENTARY NOTES

14. ABSTRACT

Results from large-scale hydraulic fluid spray fire tests have been compared with simulations of those tests using the Fire and Smoke Simulator (FSSIM) model. Using a model calibration data set, the sensitivity of FSSIM to several key inputs was evaluated; for the critical heat release rate (HRR) parameter, an adjustment factor was estimated to correct for unburned fuel. The resulting input parameters were then applied to similar data sets and the predictions compared with test data. In most cases, very good agreement was obtained. Some issues related to the use of the FSSIM graphical interface, including directions for future development, were discussed.

15. SUBJECT TERMS

Fire
Fire modeling
Large-scale test
Hydraulic fluid fire

16. SECURITY CLASSIFICATION OF:			**17. LIMITATION OF ABSTRACT**	**18. NUMBER OF PAGES**	**19a. NAME OF RESPONSIBLE PERSON**
					J.B. Hoover
a. REPORT	**b. ABSTRACT**	**c. THIS PAGE**	UL	70	**19b. TELEPHONE NUMBER** *(include area code)*
Unclassified	Unclassified	Unclassified			(202) 767-2335

CONTENTS

1.0 BACKGROUND

Over the last three years, the the Naval Research Laboratory (NRL) has conducted a series of tests to evaluate the fire performance of materials commonly found in various shipboard spaces. During fiscal years 2005 and 2006, fuel loads typical of shipboard electronic spaces [1, 2] and dry goods storage spaces [3, 4] were evaluated. One of the major goals of that work was to develop data sets suitable for use in numerical simulations of shipboard fires. In particular, we hoped to use test data to create "fuel packages" for typical types of fires which could then be incorporated into fire models. During fiscal year 2007, we have further developed this concept by using fuel load information from previous tests to perform proof-of-concept simulations, including comparison between the model predictions and the test results.

1.1 Fire Model Overview

There are two broad classes of fire models: computational fluid dynamic (CFD) models and zone models. For CFD models, the governing equations are partial differentials, that is, they include derivatives with respect to both time and space. These equations are continuous (valid at every point) but, in order to be solved with standard numerical methods, they must be discretized (converted to a form that is valid only at a set of discrete points). This set of points, called a grid, must be mapped onto the actual geometry of the problem that is to be simulated. For the types of fire models in which we are interested, grids are usually three-dimensional but, depending on the symmetry of the problem, they could be one- or two-dimensional.

In practice, the CFD methodology involves dividing the simulation domain into a large number of small cells, each of which is represented by one point on the grid. Each grid point is characterized by a set of thermodynamic properties, which typically includes temperature, pressure and concentrations of various species. The spatial resolution of a CFD model can be arbitrarily high, depending on the size of the grid spacing. Of course, there is a practical limit since, for a given geometry, a finer grid requires more cells which means that more calculations must be performed, requiring more time, a more powerful computer or both.

Zone models take a different approach. Instead of having a grid of identical cells[1], they use a small number of relatively large zones (typically, one or two per compartment), the sizes and shapes of which are determined by the dimensions of the various compartments[2]. Normally, zone models include no chemical reactions and they often use simplified physics (for example, rather than attempting to calculate the details of a fire plume, they usually use an empirical approximation). There is no spatial grid, so no spatial derivatives are required and, as a consequence, ordinary differential equations are used.

Due to the smaller number of computational points, the use of ordinary, rather than partial, differential equations and the lack of complex physics and chemistry, zone models are often able

[1] Technically, the cells in CFD models are not required to be identical. Modern CFD computer codes can use different cell sizes and shapes for different parts of the problem; they may even change the gridding dynamically, depending on the immediate requirements of the numerical methods being used.

[2] However, it is typically the case that the zones are assumed to be rectangular parallelepipeds so that they all may be represented as cubes that have been stretched or compressed to various degrees along each axis.

Manuscript approved November 1, 2007.

to run many orders of magnitude faster than CFD models. Simulations that can be run in seconds or minutes on a desktop computer using a zone model might require days or weeks on a supercomputer if done with a CFD model.

The obvious trade-off for this fast execution is the low spatial resolution of the predictions, since each compartment is represented by a single value of each property. A more subtle cost is that the absence of chemistry precludes the actual calculation of the fire behavior — in this class of model, the fire growth is a user input[3].

The general class of zone model may be subdivided into several categories, depending on how many zones are used to represent a compartment and how the compartments are mathematically coupled. The Consolidated Fire and Smoke Transport (CFAST) model, for example, represents most compartments using two zones, based on the observation that compartment fires frequently produce stratification, with a hot upper layer and a (relatively) cold lower layer.

The Fire and Smoke Simulator (FSSIM) model used in this work is a single-zone, network model. That is, each compartment is represented by only one volume, the couplings between those volumes are treated as resistances (*e.g.*, thermal resistance) to the flow of some property, and the driving forces (source terms in the equations) are provided by one or more fires.

Mathematically, this model is analogous to a three-dimensional network of electrical resistors through which current flows under the influence of various voltage sources. Just as the electrical potential of each node in the resistor network can be calculated by applying Kirchhoff's rules (see, for example, [5]), the thermodynamic values associated with each node (zone) in the network fire model can be calculated if the resistances and sources are known. In practice, the resistive terms may be estimated reasonably well from a knowledge of the properties of the construction materials (conductivity and heat capacity, for example) and the size, shape and orientation of the openings between compartments. The fire source terms may be estimated from the known heats of combustion of common fuels.

1.2 Applications of Test Data for Fire Modeling

There are two areas in which fire test data are commonly applied to fire modeling. As mentioned previously, FSSIM requires that the fire growth curves be provided by the user. Accordingly, one application of test data is to develop "fuel packages" that define the fire growth characteristics for typical classes of fuels. Reference [4] discusses the development of several such packages, based on fuel loads expected to be present in typical shipboard dry goods storage spaces. It is anticipated that these packages will be incorporated into future version of FSSIM so that users may specify an appropriate fuel load using menus or checkboxes.

A second application is to validate the model predictions by comparison with actual results. Both of these applications are critical to the acceptance of fire models for use outside of the research community. Without the availability of pre-defined fuel packages, fire modeling will not be accessible except to a small number of experts within the technical community. In the absence of

[3] Many zone models, including the one used in this work, do have the ability to restrict the fire size based on availability of oxygen.

widely accepted validation tests, the model will never be trusted enough to be used in any mission-critical situation. NRL has used full-scale test data for validation of the CFAST fire model [6, 7] in the past; the current work focuses on the use of ex-USS SHADWELL data to support validation of the FSSIM model.

1.3 The Fire & Smoke Simulator (FSSIM) Model

There are two components to the model referred to as "FSSIM" – the fire model itself and the graphical user interface (GUI) that is used to set up and run simulations. These components are discussed in this section.

FSSIM was developed by Hughes Associates, Inc. (HAI) with partial support from the US Navy. The primary documentation for the model is found in a theory manual [8] and a user's guide [9]. It is a Microsoft Windows or UNIX command line tool that accepts one or more text input file(s) and generates at least one output file, depending on the user's specifications.

The primary input file consists of a set of NAMELIST groups, which are defined as lines of text having the format:

&iden param1=a, param2=b, …, paramN=z/

where '&' and '/' are literals that start and end the line, 'iden' is a four-character string that serves to identify the type of input, 'param1', 'param2', … 'paramN' are keywords that specify particular parameters associated with the given input type and 'a', 'b', … 'z' are the values that are assigned to those parameters. A large number of NAMELIST identifiers are listed in reference [9]. However, only a few are important for our purposes and these are described in Table 1. Any lines in the input file that start with '!' are comments and are ignored. It is also possible to insert comments at the end of the NAMELIST line, because anything following the '/' terminator character is ignored.

The input file is complex, due to the large number of options and to the fact that many of the NAMELIST lines refer to other lines. In effect, HAI has implemented a relational database in the form of a single file, where each NAMELIST line is a data record that may refer to other records. As a result of the number of lines required for even moderately complex cases[4], and to the inter-relationships among these lines, it can be difficult to manually produce a self-consistent input file.

1.4 The FSSIM Graphical User Interface (GUI)

In order to make the model more accessible to inexperienced users, Mississippi State University (MSU) was funded to develop a graphical user interface (GUI) for the HAI model. As was the case for the underlying fire model, both a theory [10] and a user manual [11] were published; the latter was subsequently updated for version 2.4 of the GUI (version 1.2 of FSSIM) [12], which was used in this work.

[4] For example, the typical simulation performed as part of this work required nearly 1000 lines in the input file.

Identifier	Description
EXEC	Controls execution of the model. Includes simulation time, ambient temperature, pressure, oxygen concentration and output root file name.
JUNC	Defines mass-flow connections between compartments (such as doors, hatches and holes caused by weapons hits).
FIRE	Defines the type, location, combustion and growth properties of the initial fires.
COMP	Defines compartment dimensions, elevation, volume, initial temperature and pressure.
SURF	Defines compartment boundaries, including area, orientation, a reference to the composition of the surface and references to the two compartments which share the surface.
MTRL	Defines the properties of each material used in a surface. The thermal conductivity, heat capacity, density and surface emissivity are included.
CMPN	Defines the composition of a surface, including the number of layers, layer thicknesses and and references to the materials used.
CURV	Provides a mechanism for specifying data points, in the form of XY pairs. This may be used, for example, to build an arbitrary fire growth curve.
RNOD	Defines the nodes for a mechanical ventilation system. It includes the number of ducts connected to the node, references to the duct identifiers, loss coefficients for flow paths through the node, the node elevation and a flag indicating whether the node is a terminal.
RDCT	Defines the ducts for a mechanical ventilation system. Duct area, perimeter, length and loss coefficient are included.
RFAN	Defines the performance characteristics of a fan used in a mechanical ventilation system.
CTRL	Allows devices (such as fans, suppression systems and doors) to be activated/deactivated (opened/closed) at pre-set times or under pre-set conditions (for example, at a given temperature).
CNTR	Specifies the number of compartments, fires, junctions and other inputs. This provides a mechanism to help validate the input file.

Table 1. Key NAMELIST Identifiers for FSSIM

This list includes only those identifier that were most important for the current work. Also, not all of the available parameters are discussed for each identifier.

The MSU GUI runs on Microsoft Windows operating systems (Windows 2000 and Windows XP have been tested; it may also work on other versions of Windows). In addition to the GUI application itself, it is necessary to download and install the MySQL database (version 4.1 is recommended, although that is not the most current version available). After installing the database, you must also run a structured query language (SQL) script that initializes the database tables required by the GUI.

This system was designed to be easily installed and used by non-expert users (for example, crew members on a ship). It was also intended that the application data be difficult to corrupt — for this reason, the database is not accessible via the GUI so that the geometry of the scenarios can not be altered. Presumably, after the FSSIM/GUI package is put into service aboard a ship, any required updates will be provided by a revised SQL script that will update or replace the existing database tables.

When the GUI application is run, the user selects the desired geometry, which is then displayed and may be manipulated (including rotation, translation and zoom in/out) to make it easier to see specific hatches, doors and other design features. Ambient conditions (temperature, pressure and oxygen concentration) can be specified, individual closures may be opened or closed, the degree of holing may be defined for each surface and initial fires may be added or deleted. For each fire, the compartment, fire type (constant intensity, t^2 growth or user-defined growth) and combustion characteristics (for example, heat of combustion, heat of vaporization and species yield fractions) may be given.

After the target scenario has been completely defined, the model is run and the results are displayed as the simulation progresses. By default, the compartment temperatures are mapped to a color value and soot concentrations are mapped to saturation values so that the compartments change to yellow, orange and red as the temperature rises and become progressively darker as the smoke concentration increases. The GUI may be set to display other variables, such as oxygen concentration, instead of temperature and smoke, and the color mapping may be changed.

Although hidden from the user, running the model is actually a multi-step process. In the first step, the GUI application automatically generates the required NAMELIST lines, creates the FSSIM input file and saves that file to the hard disk. It then invokes the FSSIM model and directs it to read and execute the input file. As the model runs, FSSIM produces output files in a special, GUI-compatible format. These files are read and parsed, in real time, by the GUI application which uses the temperature and concentration data to generate the appropriate color and shading for the display.

Note that, as mentioned above, there is no mechanism for changing the geometry (*e.g.*, compartments, bulkheads, hatches and doors can not be added to, or deleted from, the model)[5]. One consequence of this design is that it is extremely difficult, verging on impossible, to use the GUI for any geometries other than the four that are provided with the program (described in Table 2).

[5] However, as note previously, there is a mechanism for setting the amount of damage for pre-defined surfaces.

We should note that this is due to the absence of any GUI tools to create or alter the database tables. The lack of such tools within the MSU application is not an absolute impediment because many tools are readily available to manipulate MySQL databases. However, the database schema is not documented and it must be assumed that it is subject to change without notice. Thus, while it would certainly be possible to reverse engineer the database schema, that probably would not be a good idea.

Geometry	Description
Confined_Space	SHADWELL/688 submarine test area.
Ship_A	Generic warship.
Building_B	Generic building with multiple rooms, long halls, conference room and high bay area.
Shadwell_Forward	SHADWELL machinery space test area.

Table 2. Geometries Provided with the Mississippi State GUI

The database that is provided with the current MSU GUI software package includes the four geometries listed. These can not be altered, nor can additional geometries be defined with the tools provided.

2.0 OBJECTIVES

The objectives of this work were to:

1. simulate selected fires from previous tests using FSSIM;
2. compare the model predictions with the experimental data; and
3. document the observed inconsistencies, if any, between the model and the actual fire results.

3.0 EXPERIMENTAL

The limited number of geometries built into the GUI application posed a problem for this work because, while we would have liked to simulate the storage space test area [3, 4], that geometry was not available in the GUI. However, the SHADWELL/688 submarine test area, shown in Figure 1, is one of the standard geometries. Accordingly, we chose to simulate several of the hydraulic spray fires that were conducted in the submarine spaces during the Hydraulic System Explosion and Fire Hazard program. The test setup and procedures are summarized in this section; more details may be found in the references [13, 14].

We selected tests HFH-10 — HFH-12 to be simulated because those tests were originally designed and configured to produce data specifically for model validation. All three used the

Hatches/Scuttles		Doors		Framebays	
ID	**Status**	**ID**	**Status**	**ID**	**Status**
H1	Open	D1	Closed	#1	Open
H2	Open	D2	Open	#2	Open
H4	Open	D3	Open	#3	Open
H5	Open	D5	Open	#4	Open
H7	Open	D6	Open	#5	Closed
H8	Open	D7	Closed	#6	Open
H9	Open	D8	Open	#7	Closed
H10	Open	D9	Open	#8	Open
H11	Open	D10	Open		
H12	Open	D11	Closed		
H13	Open	S1	Closed		
H14	Closed	S2	Open		

Table 3. Closure Configuration for Simulated Tests

The closure status of hatches, doors and framebays for tests HFH-10 — HFH-12 are given. The locations of the closures are shown in Figure 1B. Note that door D4 and hatch H3 did not exist in this configuration and the framebays are not shown in the Figure.

Fuel Property	Property Value
Composition	>99% Heavy paraffinic distillates
Absolute Viscosity (cP)	69.0 @ 40 °C; 8.4 @ 100 °C
Flash Point (°C)	246
Boiling Point (°C)	>315
Specific Gravity	0.86 - 0.87
Heat of Combustion (MJ/Kg)	42.7

Table 4. Selected Properties of ChevronTexaco 2190 TEP Hydraulic Fluid

These properties of ChevronTexaco 2190 TEP hydraulic fluid were taken from the manufacturer's product data sheet and the Material Safety Data Sheet.

closure configuration shown in Table 3. The test fires were located in the torpedo room and the fuel was ChevronTexaco 2190 TEP hydraulic fluid (MIL-PRF-17331J [15]). Properties of 2190 TEP are given in Table 4.

In the following section, we discuss the experimental setup, starting with the overall configuration of the test area and progressing to the details of the instrumentation and the data acquisition system.

3.1 SHADWELL/688 Test Area

The SHADWELL/688 test area, located in the port wing wall of ex-USS Shadwell, represents the forward compartment of a *USS Los Angeles* (SSN 688) class attack submarine. As seen in Figure 1, it includes five decks and 17 spaces. The hatch and door numbers are not consecutive because the numbering scheme was developed for a previous test series and door D4 and hatches H3 and H6 were subsequently eliminated.

The fan room, CPO living space and storeroom were isolated from the actual test area by the closure of doors D1, D7 and D11. In the case of the fan room, this was necessary to ensure that the ventilation system worked correctly (the fan room is a plenum that is an active part of the ventilation system). The other two spaces were isolated in order to protect the instrumentation node rooms that are located within them. Similarly, hatch H14 was closed to protect wiring that is routed through the bilge in that area.

There are eight ducts (for clarity, these are not shown in Figure 1) connecting the main deck with the third deck. These ducts simulate the connections that bypass, via the framebays, the wardroom and crew living spaces on SSN 688 class submarines. Four of these ducts (two port and two starboard) connect the torpedo room with the combat systems space, two (starboard) provide a direct path between the laundry room and the control room and the last two (port) go from the laundry passageway to the control room. For these tests, all except the last two were open.

Bete P24 (90° solid cone pattern) nozzles were selected for these tests. At our request, Bete calculated the size distribution parameters for hydraulic fluid sprays using the specific gravity and viscosity from Table 4. The resulting estimated size distribution parameters are given in Table 5 [16].

Press. (psi)	Dv(10)	Dv(50)	Dv(90)
1000	50	84	130
1500	44	74	110

Table 5. Estimated Size Distribution for Bete P24 Nozzles with 2190 TEP Hydraulic Fluid

Estimated droplet diameters, in microns, for the 10th, 50th and 90th percentiles (by volume) at nozzle pressures of 1000 and 1500 psi. These values were calculated by the nozzle manufacturer (Bete Fog Nozzle), using proprietary software, for 2190 TEP fluid parameters.

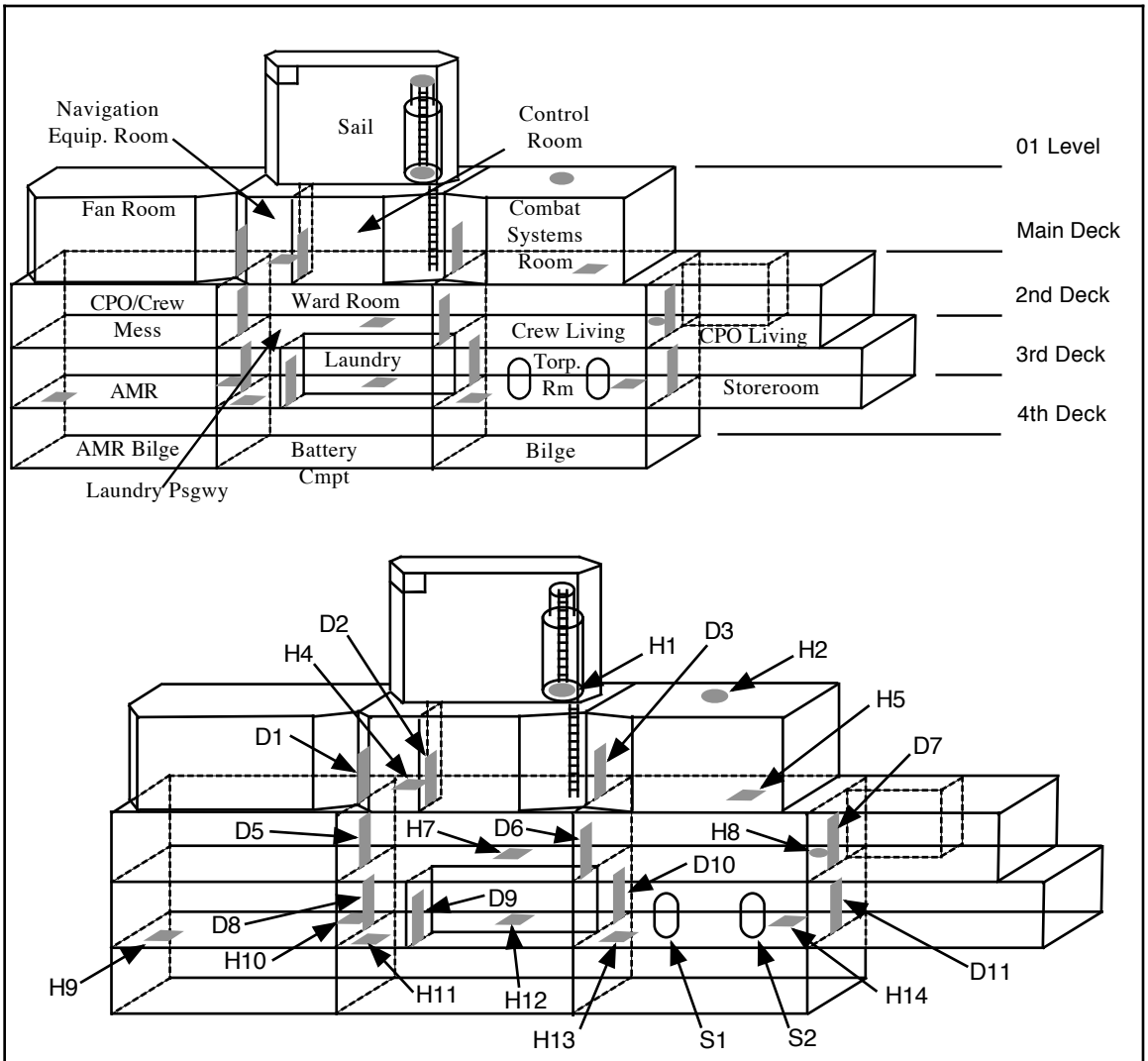

Figure 1B. SHADWELL/688 Test Area Compartments and Closures

The geometry of the SHADWELL/688 area is shown, with the compartments (upper) and and closures (lower) labeled. For clarity, the frame bays discussed in the text are not shown. Frame bays #1 - #4 connected the torpedo room and the combat systems space; #5 and #7 connected the laundry passageway and the the control room; #6 and #8 connected the laundry room and the control room. Note that the decks are labeled using the SHADWELL designations, not the nomenclature used on *USS Los Angeles* class submarines.

Fuel flow was controlled by the pressure and the nozzle characteristics. For the tests in question, a single nozzle was used, operating at a pressure of approximately 1000 psi; this was expected to produce a flow rate of approximately 2.0 liters/min (0.54 gpm) for an estimated heat release rate (HRR) of 1.2 MW.

3.2 Instrumentation

For this work, our primary interests were the temperatures in the fire compartment (torpedo room) and the habitability of the control room and combat systems space. Habitability is largely determined by the air temperature, concentrations of oxygen and toxic gases and the visibility. Accordingly, the primary instrumentation for these tests were the thermocouples in the torpedo room, control room and combat systems space, the gas sample loops in the torpedo and control rooms and the control room optical density meters (ODMs). Additional thermocouples were located in the crew living space, the laundry room and the laundry passageway. The locations of the instruments in these compartments are shown in Appendix A; more detailed descriptions of the instruments are given below.

3.2.1 Thermocouples

The torpedo room and crew living space each had four thermocouple trees, the control room[6] and the laundry passageway had three and the combat systems space and laundry room each had two. Each tree had five thermocouples at approximately 0.5 m (1.7 ft.) vertical intervals from 0.5 m (1.7 ft.) to 2.5 m (8.2 ft.). Some trees had an additional thermocouple located at an elevation of 5.0 centimeters (2.0 in.).

In addition, a thermocouple was placed above the spray nozzle (near the overhead) in the torpedo room. Because the flame impinged on this thermocouple during most test, it was not useful for measuring ambient temperatures but did provide verification of ignition and extinguishment.

3.2.2 Gas sampling

Two of the three available gas sample loops were installed in the port, forward portion of the control room, one at an elevation of 0.46 m (1.5 ft.) and the other at 2.3 m (7.5 ft.). To monitor the oxygen availability near the fire location, the third gas sampler was placed in the torpedo room 1.0 m (3.3 ft.) above the deck and 0.6 m (2.0 ft.) aft of the forward bulkhead.

3.2.3 Optical density meters

Two ODMs were located in the control room, near the gas sampling intakes, at elevations of 1.0 m (3.3 ft.) and 2.0 m (6.6 ft.). These provided an indication of optical transmission, which is related to visibility by Equation 1 [17][7]

$$\text{Vis} = 3/K \qquad \text{Eqn. 1}$$

[6] The control room was divided into two regions, the control space (which had two thermocouple trees) and the navigation equipment space (which had one). For convenience, the term “control room” refers to both.

[7] This equation applies to reflecting (as opposed to light emitting) signs having high contrast.

where Vis is the approximate visibility (meters) and K is the extinction coefficient (m^{-1}). The extinction coefficient, a measure of how much light is absorbed over a given path length, may be obtained from the transmission equation

$$T_f = \exp(-K\, l) \qquad \text{Eqn. 2}$$

where T_f is the fractional transmission (dimensionless) over the path length l (meters).

3.3 Data acquisition and analysis

The data acquisition system used in these tests was a MassComp computer running a version of Unix. Two custom, software-controlled 200-channel digitizers were used to scan the inputs at one Hertz, store the data on a hard drive and display selected data in real time. At the completion of the test, the data were converted to text format and transferred to a personal computer for off-line analysis.

Since FSSIM is a single-zone model, it was necessary to convert multiple-point data measurements into single values representative of the entire compartment. This was done by averaging the valid[8] data for each compartment. In the case of air temperature measurements, the data were first normalized to a constant initial temperature (25 °C) to correct for different initial ambient temperatures and make comparisons among the tests easier.

4.0 SIMULATIONS

Although the FSSIM model is relatively easy to use, it does require a certain amount of work to correctly specify the scenario and to set up the proper initial conditions. In some cases, there may be more than one possible way to configure the model. Issues related to model setup are discussed in the following sections.

4.1 Model Calibration

Model calibration involves tuning some of the FSSIM parameters so that the model more faithfully represents actual test conditions. The primary issue is that FSSIM, like other zone models, requires that the fire growth history be provided as an input. This means that the heat release rate and the carbon monoxide, water vapor and set yields[9] must be specified, as functions of time, prior to execution of the model. However, these parameters, especially the product yields, depend heavily on the details of the combustion which can not be known *a priori*.

Thus, we are faced with a contradiction — the model can't be run unless the fire history is known; the fire history can't be known until the time-dependent combustion conditions are known; the combustion conditions can not be known until the model is run.

[8] Some data were rejected due to instrument malfunctions.

[9] Carbon dioxide yield may also be given but, usually, it is not because that would over specify the problem and could lead to numerical errors.

Our solution to this problem was to estimate the likely range of values for the fire parameters, run the model and adjust the parameters as necessary to fit a typical scenario. Those parameters could then be used to produce reasonable approximations for other, similar, fire scenarios.

Data from test HFH-10 were used to perform the model calibration, the resulting parameters were then used to simulate tests HFH-11 and HFH-12 and the predictions from the latter two tests were then compared with test data in order to estimate the accuracy of the model for this type of fire scenario.

4.1.1 Development of the Base Simulation

The initial phase of the process was to develop a base fire simulation, using the best available information about the scenario. It was found that, even for the SHADWELL/688 area, the GUI had several limitations that needed to be addressed before we could simulate the fires. First, there were two safety doors, (labeled 'S1' and 'S2' in Figure 1B) that were not included in the GUI database. One of these doors (S2) was open during tests HFH-10 - HFH-12 and provided direct access to the torpedo room from the welldeck. In order to properly simulate the actual ventilation conditions, it was necessary to add this door to the model geometry.

Second, there were four framebays that connected the torpedo room and combat systems and four more that connected the laundry/laundry passageway with the control room. The GUI includes the framebays[10], but only permits them to be opened or closed as a group. In our tests, six of the framebays were open and two were closed, so we had to manually adjust these closures in order to properly account for the transport of smoke and toxic products from the third deck to the main deck, bypassing the second deck.

To address these limitations, we performed the initial modeling in two steps. First, the fire parameters and hatch and door closures were set, using the GUI, and the model was run. The output file produced by the GUI program during this step (which included all of the compartments, surfaces, junctions and other required FSSIM inputs) was then manually edited to add the safety door and to set the framebay closures as appropriate to the actual test scenario. It was also necessary to change the &CNTR line to reflect the correct number of junctions, ventilation nodes and ducts — without this, FSSIM rejects the input file as invalid. The manual changes that were applied to the input file are summarized in Table 6.

The ambient temperature, pressure and oxygen concentrations were set to the default values of 298.15 K (25 °C), 101,325 Pa (one atmosphere) and 23 mass percent (21 volume percent). Parameters related to the combustion properties of the fuel were specified as in Table 7. The values shown were obtained from various sources, as explained below.

The fire was confined to the torpedo room and, because the fuel flow was kept constant during the test (by maintaining the fuel pressure at a constant value), we know that the fire was essentially constant. The heat of combustion of the fuel was taken from the data provided by the manufacturer of the hydraulic fluid (ChevronTexaco) and the heat release rate for the test was

[10] Because the framebays connect non-adjacent compartments, they must be represented as ducts and nodes in the mechanical ventilation system, rather than as simple junctions.

determined from the mass loss of the fuel reservoir over the run time of each test. For test HFH-10, this was 0.022 kg/sec which, using the given heat of combustion, corresponds to 0.94 MW. This is in reasonable agreement with the value that was estimated based on the nominal performance of the Bete P24 nozzle (1.2 MW).

Change	Description
Add &JUNC	Door S2
Delete &RNOD 111	Port control room terminal #1
Delete &RNOD 112	Port laundry passageway terminal #1
Delete &RNOD 113	Port control room terminal #2
Delete &RNOD 114	Port laundry passageway terminal #2
Delete &RDCT 52	Port duct #1
Delete &RDCT 53	Port duct #2
Modify &CNTR	njucn = 24, nnode = 63; nduct = 54

Table 6. Input File Modifications for the Base Scenario

Each framebay is represented by the combination of two &RNODs (the ventilation terminals in the control room and laundry passageway) and one &RDCT (the connecting duct segment). The number of junctions (njunc), ventilation nodes (nnode) and ducts (nduct) were changed to reflect the added &JUNC and the deleted &RNOD and &RDCT lines.

Parameter	Value
Compartment	Torpedo Room
Fire Type	Constant
Heat of Combustion	42.7 MJ/kg
Heat Release Rate	940 kW
Heat of Vaporization	182.5 kJ/kg
Pyrolysis Temperature	590 K
Water Yield	1.345 (kg water/kg fuel)
Carbon Monoxide Yield	0.012 (kg CO/kg fuel)
Soot Yield	0.042 (kg soot/kg fuel)
Carbon Dioxide Yield	1

Table 7. Fuel Combustion Properties for the Base Scenario

The derivation of these parameter values is discussed in the text. Note that using -1 as the carbon dioxide yield tells FSSIM to calculate the species concentration using the mass balance of carbon in all species.

The heat of vaporization for the fuel was estimated from the known values of paraffinic hydrocarbons. As shown in Figure 2, heat of vaporization was plotted as a function of carbon number for various alkanes and the curve was extrapolated to the C_{18} - C_{19} range, which is a typical chain length for hydrocarbons having boiling points similar to that of 2190-TEP (see Table 4). The resulting value, 182.5 kJ/kg, was used for these simulations. The pyrolysis temperature, estimated as 590 K, was based on the assumption that the fluid could begin to undergo thermal decomposition slightly above the boiling point.

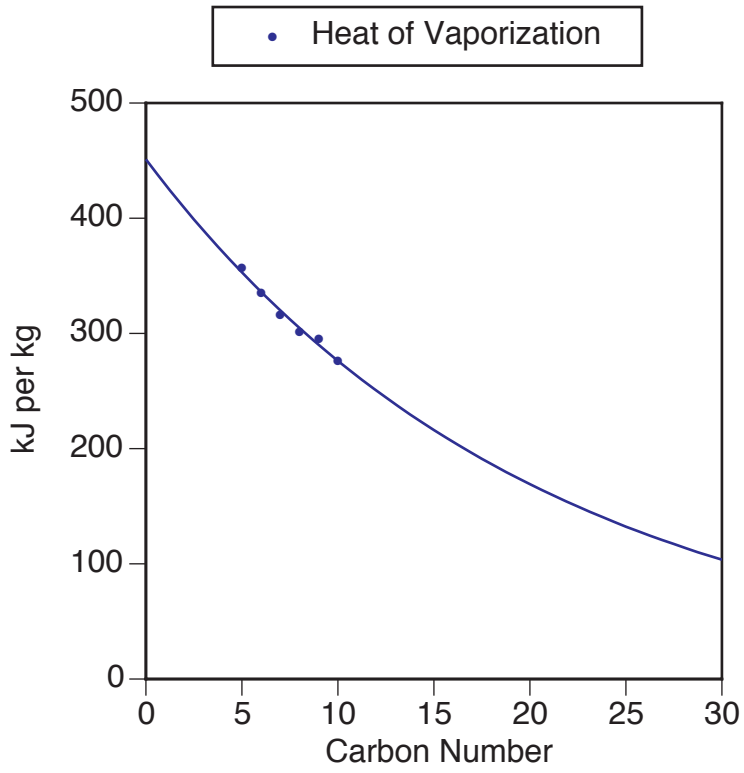

Figure 2. Estimation of Heat of Vaporization

The heat of vaporization (H_v) for hydraulic fluid was estimated by extrapolation from the known values of other hydrocarbons. The effective carbon number for hydraulic fluid was assumed to be between 18 and 19.

The water vapor yield factor was calculated by assuming that the hydraulic fluid could be approximated as a C_{18} - C_{19} alkane and that it would be completely oxidized to carbon dioxide and water. We then calculated the amount of water produced per unit mass of fuel consumed and got an estimated yield of 1.345 kg H_2O/kg fuel. Yields for carbon monoxide, soot and carbon dioxide were left at their default values. Note that the default for carbon dioxide, -1, is not really a yield ratio; it is a flag that tells FSSIM to calculate carbon dioxide production from the carbon mass balance. If an actual yield had been given, the problem would have been over-specified and the mass balance criterion could have been violated due to roundoff errors.

In the following sections, we discuss the input parameter tuning that was done to improve the agreement between the HFH-10 test data and the test scenario. For each parameter, we started with the original baseline and modified one parameter at a time.

4.1.2 Heat Release Rate

Using the simulation parameters discussed above, the predicted torpedo room air temperature was compared with the measured mean temperature, as shown in Figure 3. The agreement is relatively good, but the simulations consistently over-predicted the observed temperatures.

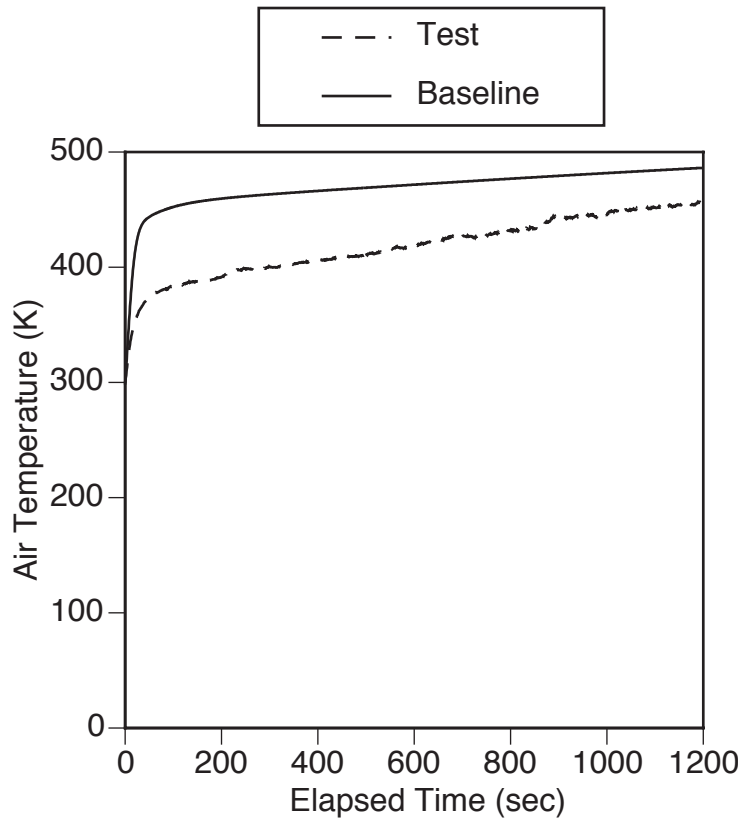

Figure 3. Comparison of Baseline Simulation and Experimental Torpedo Room Air Temperatures

The experimental mean air temperature for the torpedo room is compared with the baseline simulation, which used the parameters described in the text. Two types of comparisons were then made: air temperatures and visibility. Ideally, we would have liked to make both comparisons for the torpedo room so that errors related to soot transport would be minimized. Unfortunately, there were no ODMs in the torpedo room, so we had to rely on visibility measurements made in the control room.

It had been observed that there was a film of hydraulic fluid on the torpedo room deck after each test and that there often was unburned fluid in the pan below the nozzle. These were indications that some portion of the fuel did not burn, which is expected to reduce the temperatures. In order to estimate the magnitude of this effect, a series of additional simulations were run using the same parameters as the baseline, except that the HRR was reduced by up to 40%. Figure 4 shows the results of these changes. As may be seen, lower HRR values produced a better fit to the actual test data. Based on these results, it was estimated that approximately 35% of the fuel did not burn and that an HRR correction factor of 0.65 should be applied.

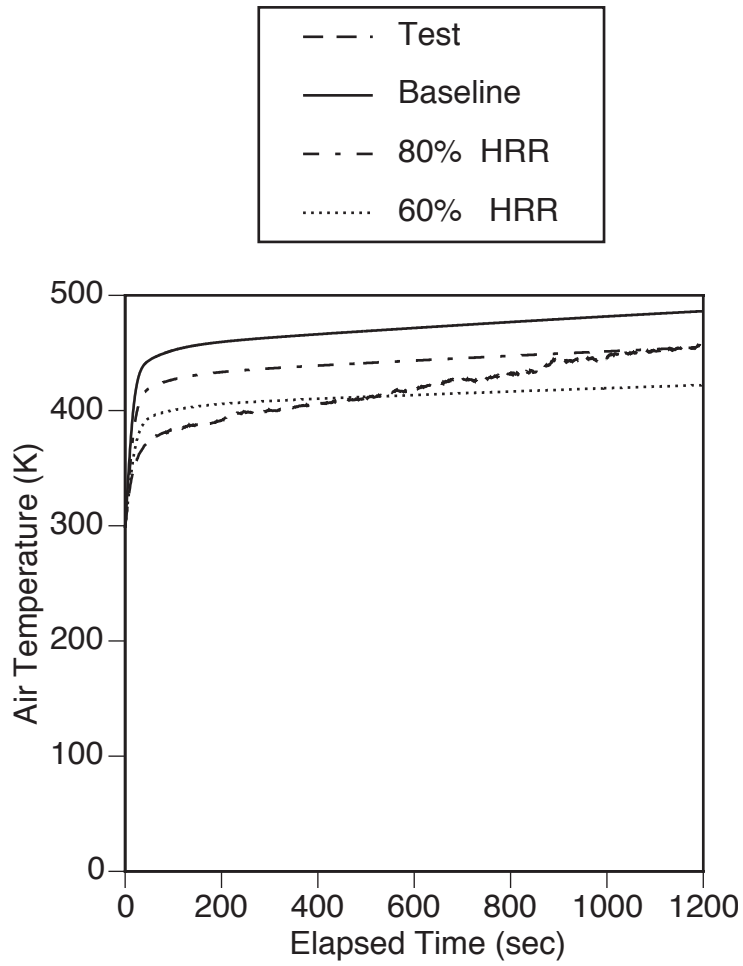

Figure 4. Effects of HRR Variation on Torpedo Room Air Temperatures

Simulation results obtained with reduced heat release rate input, relative to the baseline simulation, were found to better approximate the observed temperatures.

4.1.3 Soot Yield

Soot is known to significantly affect temperature predictions in some fire models [7] because it can cause large changes in the effective emissivity of the smoke layer which, in turn, controls the amount of energy radiated from, or absorbed by, the layer. The sensitivity of FSSIM predictions to soot concentration was not known. Accordingly, we varied the soot yield parameter from zero to twice the default value.

Variation of the soot yield parameter had almost no effect on the torpedo room air temperatures, as seen in Figure 5, where the difference at the end of the 1200 second simulation time amounted to about ±0.4% of the baseline predicted temperature.

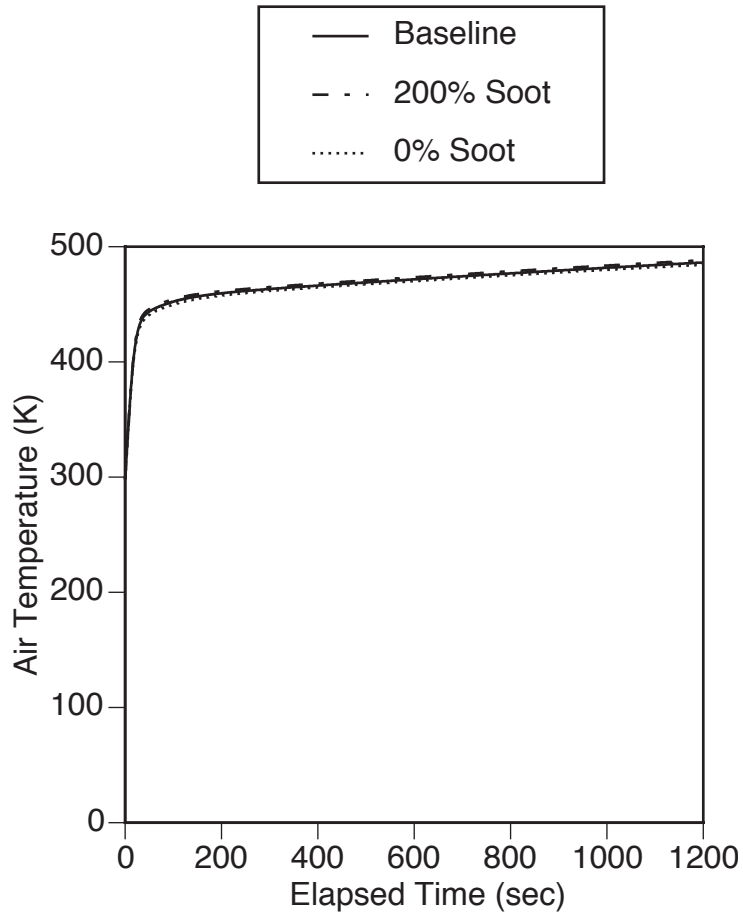

Figure 5. Effects of Soot Yield Variation on Predicted Torpedo Room Air Temperatures

Changing the soot yield factor by 100% in either direction had very little effect on the torpedo room air temperature predictions.

In order to compare the visibility data, it was necessary to convert the test data and model results to common units — the test values were reported as percent transmission and the simulation outputs were in units of soot mass per kilogram of air. The conversions were performed as described below.

For the test data, we combined Equations 1 and 2 and rearranged the result to give

$$\text{Vis} = -3\, l \,/\, \ln(T_p/100) \qquad \text{Eqn. 3}$$

where l, the path length, is one meter for our ODM instruments and T_p is the optical transmission in percent.

In the case of the simulation data, the extinction coefficient is given by

$$K = k\,[M] \qquad \text{Eqn. 4}$$

where the specific extinction, k, is the effective cross sectional area of the material per unit mass of material (m^2/kg aerosol) and [M] is the density of the aerosol suspension[11] (kg aerosol/m^3 air).

We may express the mass fraction of soot, X_{soot} (kg soot/kg air), in terms of the densities of the soot aerosol and air

$$X_{soot} = [M_{soot}] \,/\, [M_{air}] \qquad \text{Eqn. 5}$$

where $[M_{soot}]$ is the mass of soot per unit volume of air and $[M_{air}]$ is the mass of air per unit volume of air. If we assume that the air may be approximated as an ideal gas and that its composition is not significantly different from that of clean air, we may apply the ideal gas law to get

$$[M_{air}] = PW_{air} \,/\, RT \qquad \text{Eqn. 6}$$

where P is the air pressure, W_{air} is the molecular weight of air, R is the universal gas constant and T is the air temperature. Substituting Equations 4, 5 and 6 into Equation 1, we have

$$\text{Vis} = 3RT \,/\, k\, X_{soot}\, PW_{air} \qquad \text{Eqn. 7}$$

and, combining constants, we get

$$\text{Vis} = 0.09955\, T \,/\, X_{soot}\, P \qquad \text{Eqn. 8}$$

[11] Note that this is the mass of suspended material per volume of air, which is <u>not</u> the same as the density of the soot particles (mass of soot per unit volume of particles).

where we have used 8700 m^2/kg[12] as the value of k, the specific extinction coefficient for carbonaceous soot.

Figure 6 shows the comparison of predicted versus observed visibility for the control room. Note that the lowest soot yield used was 10% of the baseline; this was because the visibility is always infinite when the soot yield is zero. The default soot yield (0.042) somewhat under-predicts visibility (over-predicts soot concentration). Reducing the yield parameter from this baseline to 0.004 resulted in predictions that are more consistent with the data. Increasing the yield above the baseline by a factor of two made relatively little difference in the results.

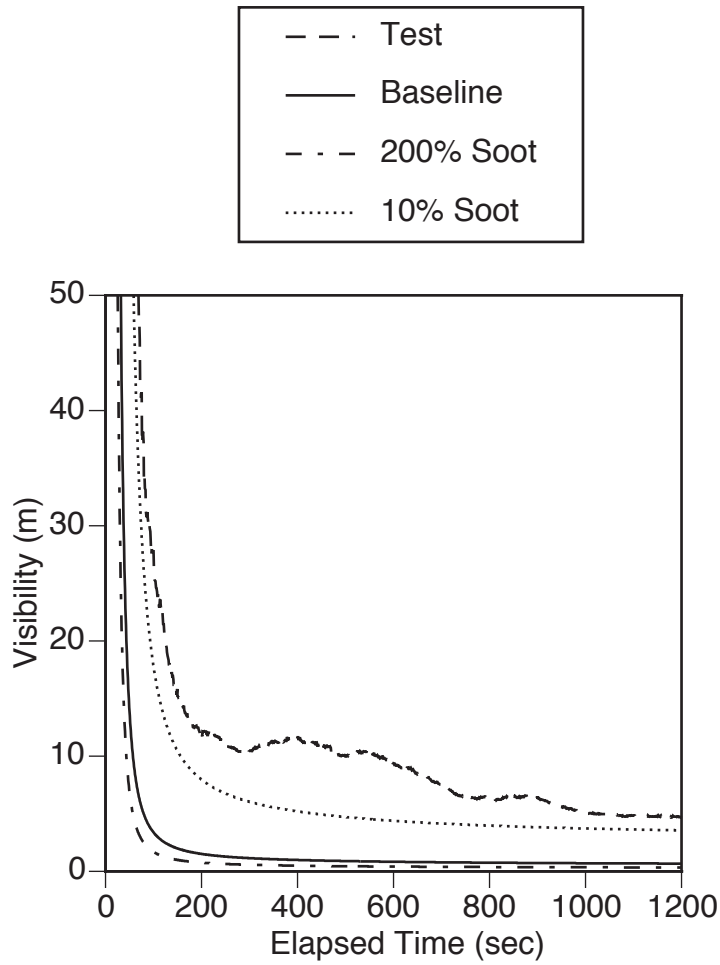

Figure 6. Effects of Soot Yield Variation on Control Room Visibility

Visibility is sensitive to the presence of soot but is not strongly dependent on the amount of soot, so long as it is greater than zero.

[12] This is the value used internally by FSSIM and by the GUI interface to convert from soot mass loading to visibility.

4.1.4 Carbon Monoxide Yield

Typically, carbon monoxide is such a minor constituent of the atmosphere that even a large fractional change in concentration represents a relatively small amount of carbon and oxygen; therefore, it has little impact on the concentrations of oxygen, carbon dioxide or soot [18]. Also, carbon monoxide has relatively little effect on temperatures because it does not contribute to the

emissivity of the gas layer. However, due to the toxicity of carbon monoxide, even small concentrations can have a major impact on the habitability of a space. Thus, we wanted to investigate the sensitivity of the FSSIM results to variations in the carbon monoxide yield input.

To this end, we ran multiple simulations in which the carbon monoxide yield was varied from zero to twice the default value. Figure 7 shows the expected, approximately linear, relationship between predicted carbon monoxide concentration and the carbon monoxide yield parameter.

In Figure 8 and Figure 9, we show that the carbon monoxide parameter has virtually no effect on the predicted torpedo room oxygen concentration or air temperature. Both of these results are to be expected, given that the carbon monoxide production has only a second order effect on the concentrations of other species. The default yield factor appears to be reasonable for carbon monoxide.

4.1.5 Closures

It was mentioned previously that the GUI was used to set the state of the closures. One aspect that was not discussed was the difference between hatches and scuttles. FSSIM makes no distinction — all openings between adjacent compartments are specified using the &JUNC keyword. However, the GUI does distinguish between hatches and scuttles and permits their closure states to be set separately.

For some closures, this is only a semantic difference. For example, H1 and H2 are actually scuttles but, so long as the dimensions of the openings are properly specified, this makes no difference to the model. On the other hand, each of the hatches H9 - H14 incorporates a scuttle as part of the hatch assembly; it was found that the GUI does not properly handle this situation — they are treated as if they were completely independent entities. Thus, the scuttle area is counted twice if both the hatch and the associated scuttle are specified as being open in the GUI.

In order to estimate the amount of error that might result from this type of mistake, we compared the results of simulations using the default baseline configuration (hatches and scuttles open) with simulations in which only the hatch was open. The results, shown in Figure 10, indicate that for this simulation, there is a small but detectable difference in the predicted torpedo room air temperatures, depending on whether the scuttles were open (incorrect area) or closed (correct area). Note that the difference in area is approximately 0.16 m^2 per hatch (a total of 0.82 m^2 for all five hatches).

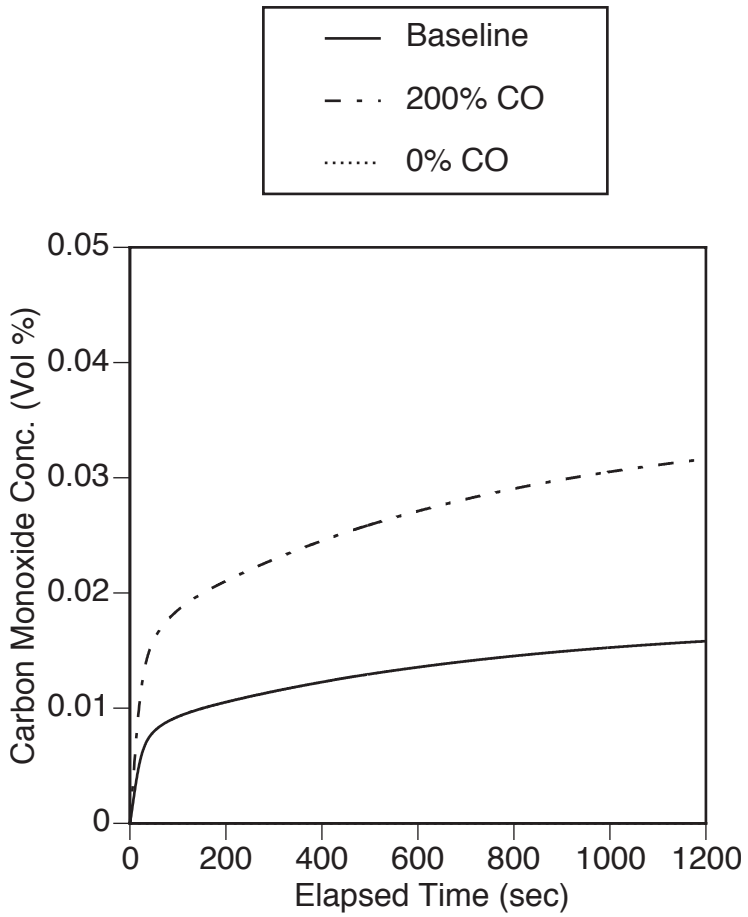

Figure 7. Effects of CO Yield Variation on Predicted Torpedo Room Carbon Monoxide Concentrations

The concentration of carbon monoxide is approximately linearly related to the value of the carbon monoxide yield parameter. As expected, the carbon monoxide concentration is identically zero when the yield is set to zero — for this case, the plot line is not visible because it is coincident with the x-axis.

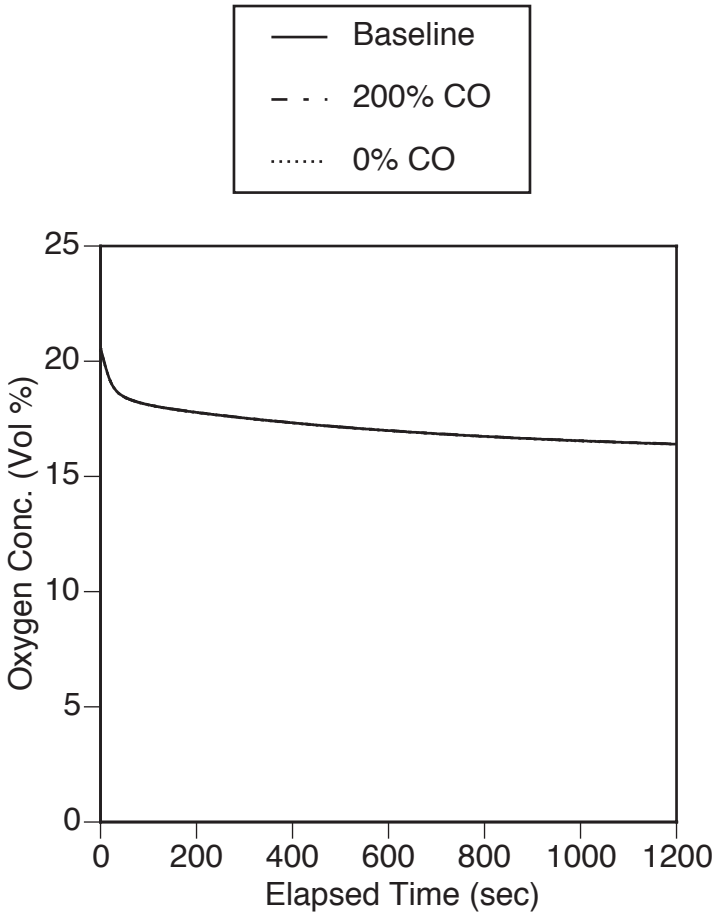

Figure 8. Effects of CO Yield Variation on Predicted Torpedo Room Oxygen Concentrations

Variations in the carbon monoxide yield parameter had no visible effect on the predicted oxygen concentration — all three plots were superimposed.

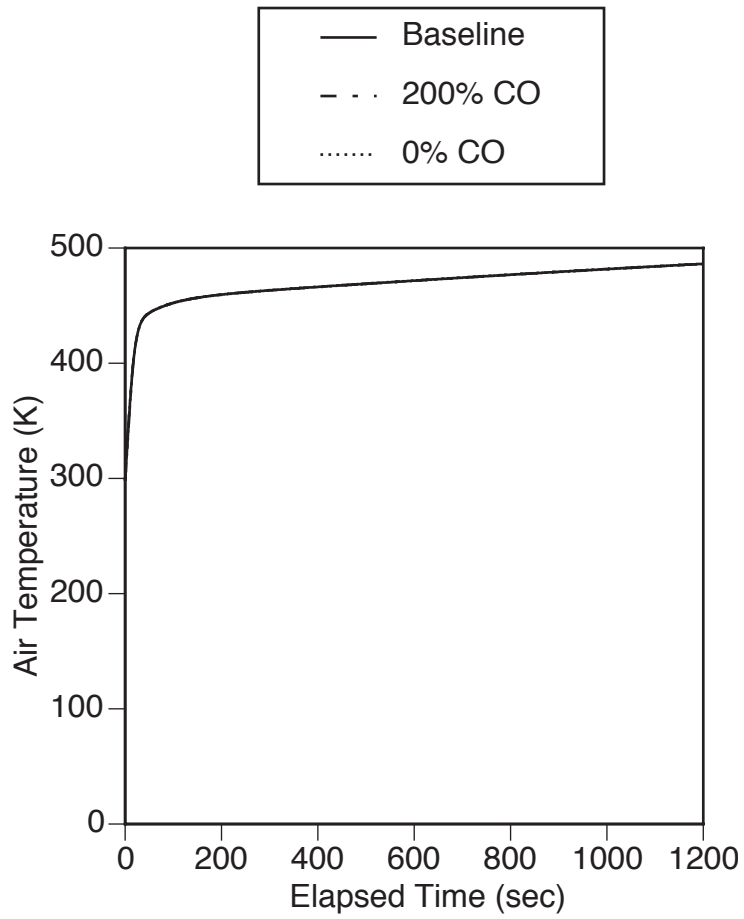

Figure 9. Effects of CO Yield Variation on Predicted Torpedo Room Air Temperatures

The torpedo room air temperature predictions were independent of the carbon monoxide yield. As in the case of oxygen concentrations, the three plots were indistinguishable.

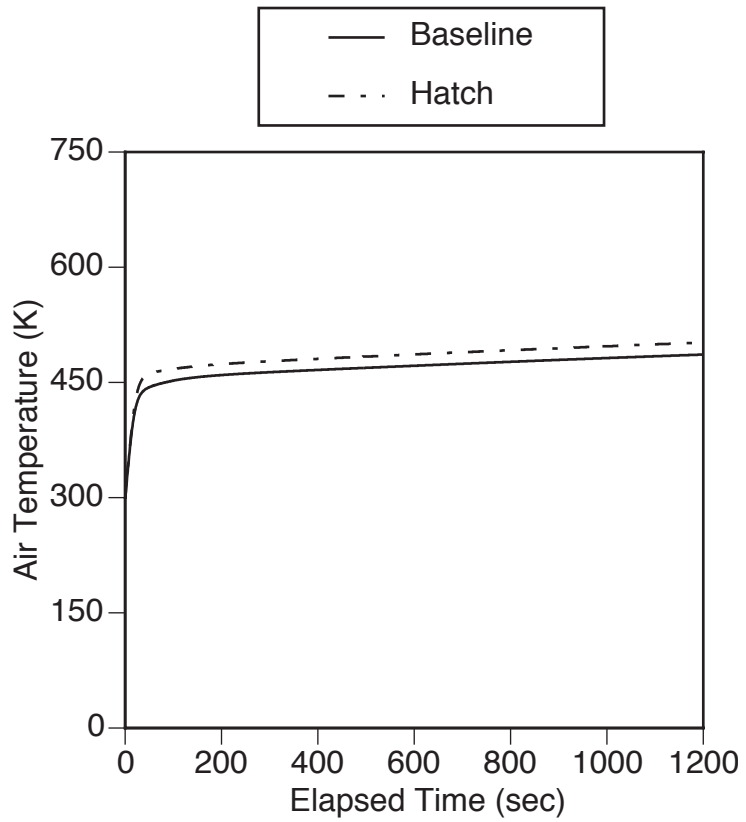

Figure 10. Effects of Closure Settings on Torpedo Room Air Temperatures

Changing the closures of H9 - H13 from Baseline (both hatch and scuttle open), to Hatch (only hatch open) has a small but noticeable affect on the predicted torpedo room air temperatures.

4.2 Test Simulations

Based on the results of the model calibration simulations, we chose to use the parameter values given in Table 8 for the test simulations of tests HFH-11 and HFH-12. In the following sections, we discuss the model predictions for the torpedo room, control room and combat systems space. Plots of additional results are included in Appendix B and Appendix C for HFH-11 and HFH-12, respectively.

It is important to recall that the FSSIM model uses a single zone approximation. This can cause problems when comparing the predictions with actual data because the data are point measurements and the model outputs are implicit averages over the entire compartment. In the case of air temperature measurements, where there were many thermocouples in each compartment, we would expect that the experimental data would provide a reasonable approximation of the actual compartment mean temperature. However, for measurements of gas concentrations and visibility, there were few sample points and, therefore, it is less likely that the data were a good representation of the mean conditions.

Parameter	Value
Heat Release Rate	65% of nominal HRR
Soot Yield	0.004 (kg soot/kg fuel)
Carbon Monoxide Yield	0.012 (kg CO/kg fuel)
H9 - H13 Closures	Hatches only

Table 8. Adjusted Input Parameters

These model input parameters, derived from the model calibration results, were used for the remaining simulations.

4.2.1 Test HFH-11

Air temperatures for the torpedo room, control room and combat systems space are shown in Figures 11 - 13, respectively. The model somewhat over-predicts the temperature in all three compartments, with the agreement in the fire compartment being the worst. The trends agree with the test results — the highest temperatures are in the torpedo room, the next highest in the combat systems space (which was directly connected to the torpedo room via the frame bays) and the control room temperatures were slightly lower than those in combat systems.

Figure 14 shows the carbon monoxide concentration in the torpedo room and Figure 15 shows that in the control room. The data for the torpedo room were bad, due to an instrument failure. However, for the control room, the agreement between the test and the model was reasonably good, although the model did over-predict the actual conditions by about 50%.

The torpedo room and control room oxygen concentrations are shown in Figure 16 and Figure 17, respectively. The agreement in the control room is excellent, while that in the torpedo room is

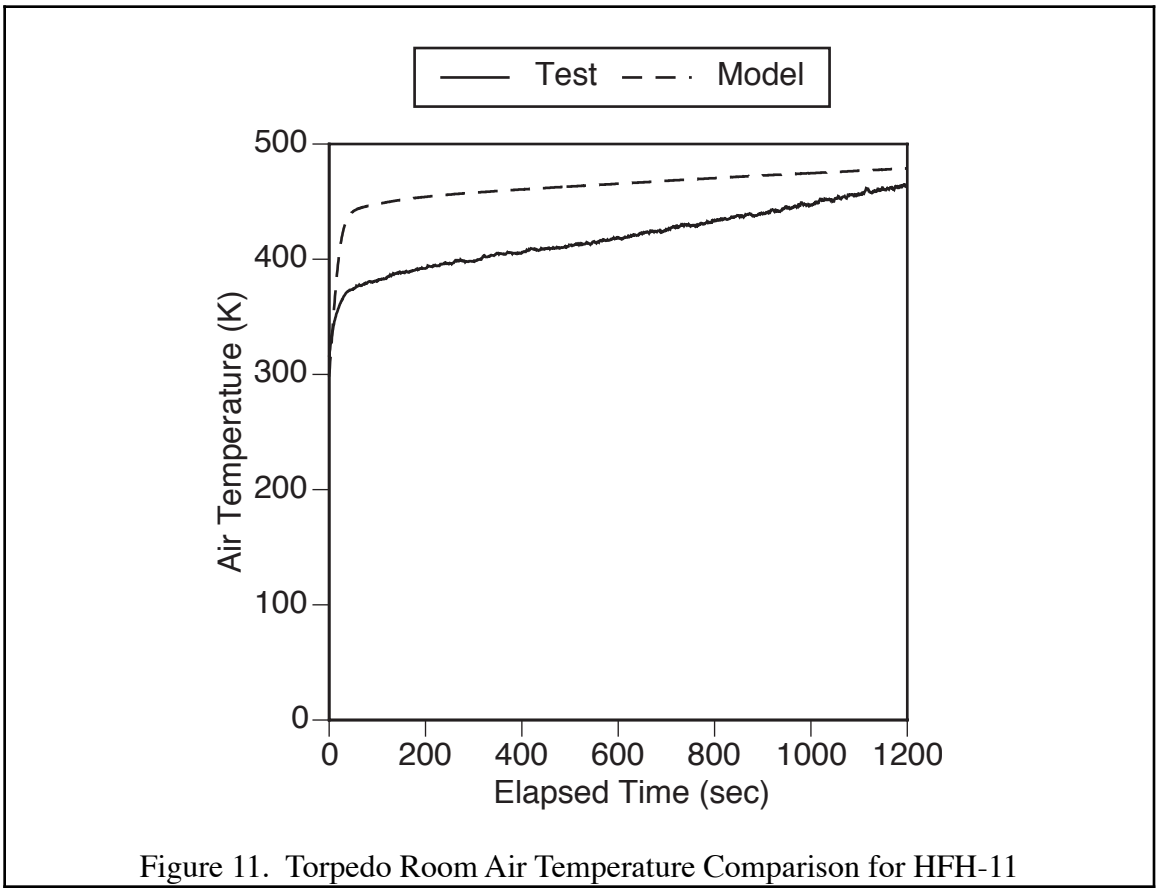

Figure 11. Torpedo Room Air Temperature Comparison for HFH-11

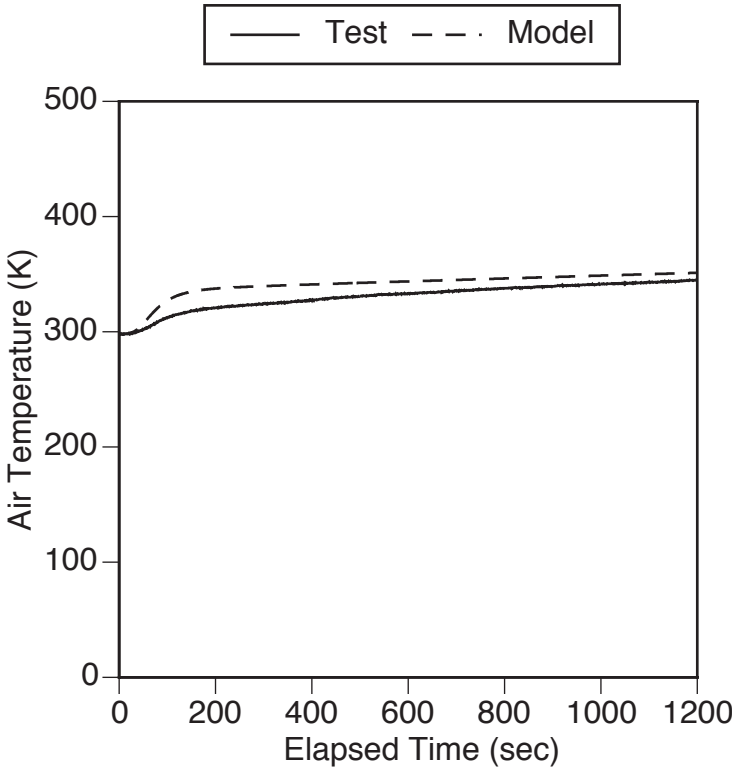

Figure 12. Control Room Air Temperature Comparison for HFH-11

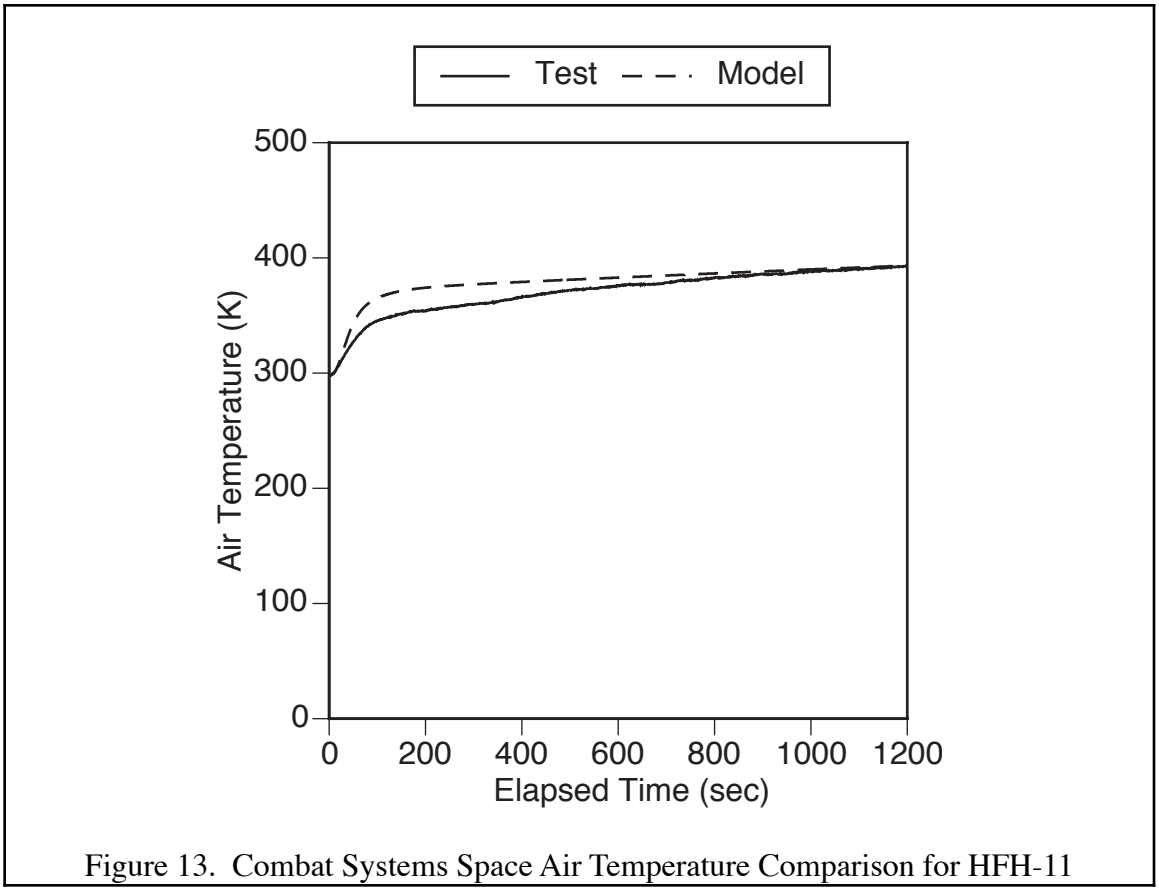

Figure 13. Combat Systems Space Air Temperature Comparison for HFH-11

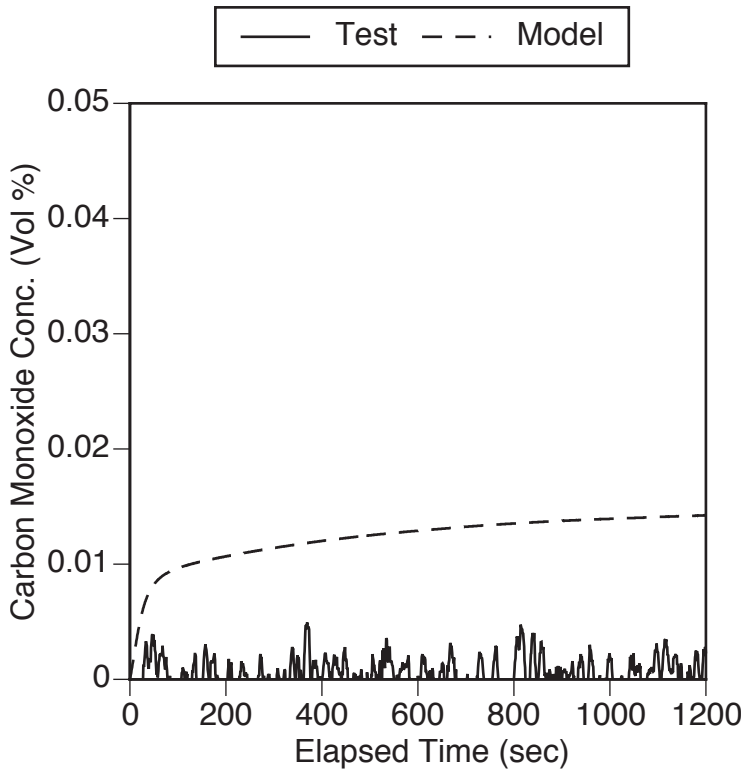

Figure 14. Torpedo Room Carbon Monoxide Comparison for HFH-11

Due to an instrument malfunction, no useful torpedo room carbon monoxide data were obtained for this test.

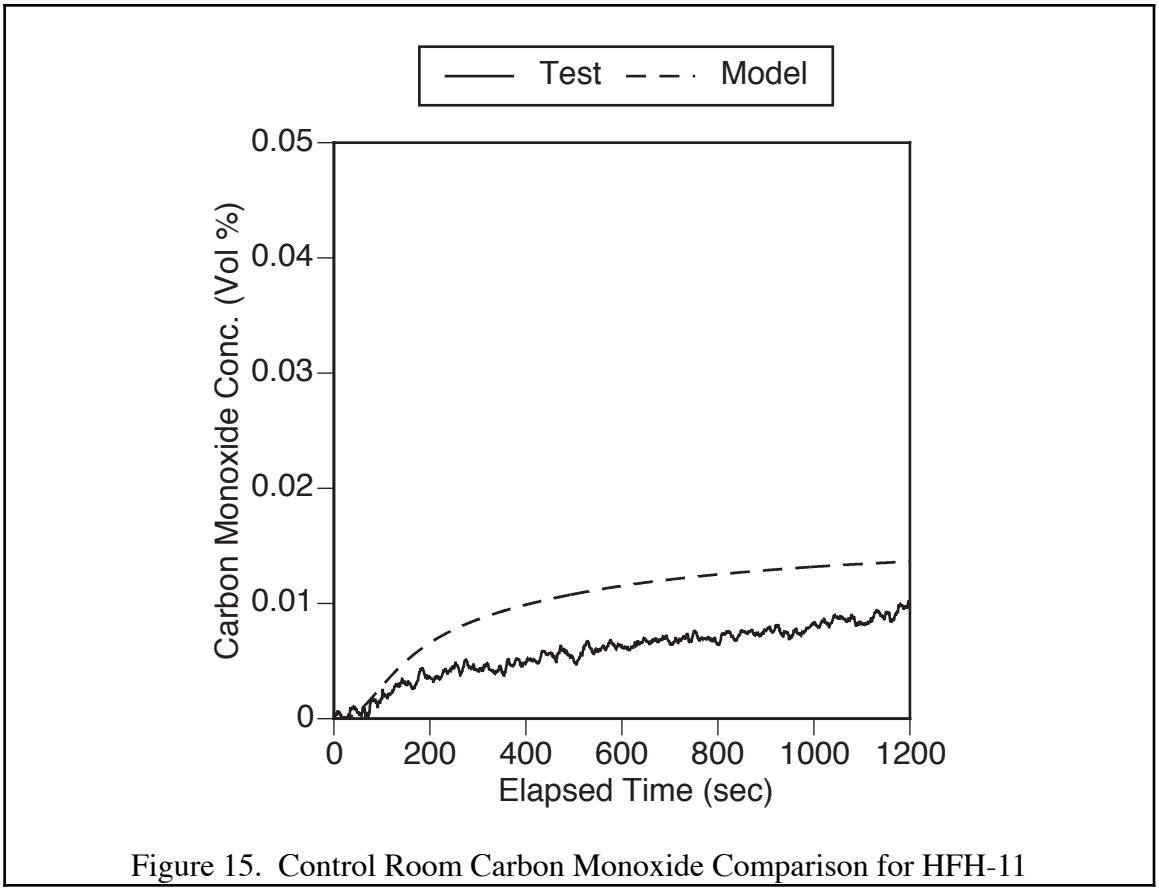

Figure 15. Control Room Carbon Monoxide Comparison for HFH-11

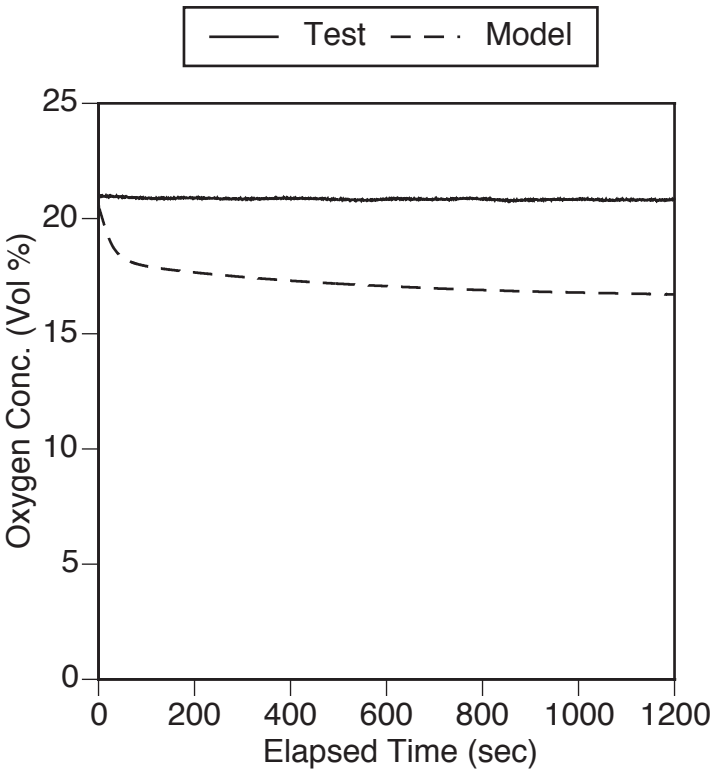

Figure 16. Torpedo Room Oxygen Comparison for HFH-11

Due to the location of the gas sampling point, the measured oxygen concentrations were not representative of the actual compartment average values in the torpedo room.

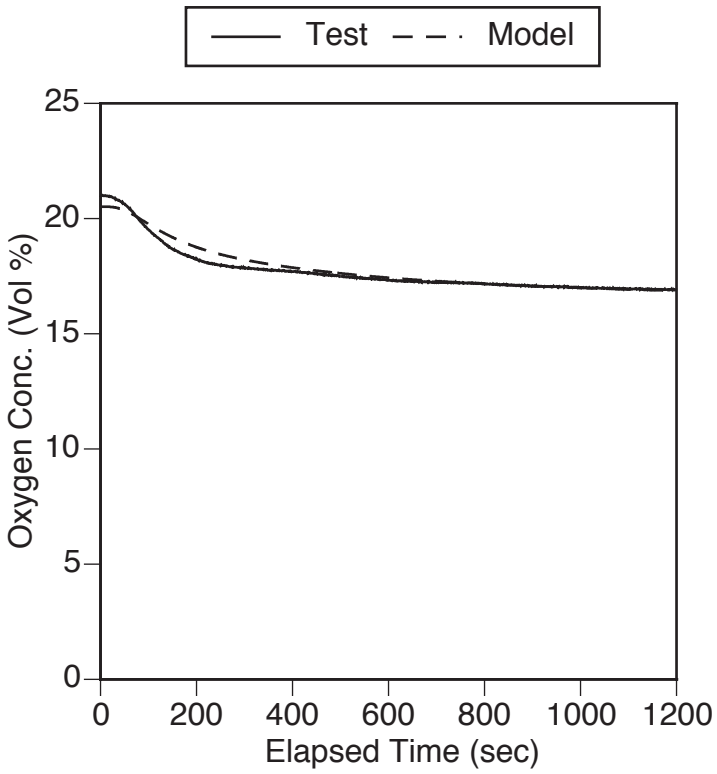

Figure 17. Control Room Oxygen Comparison for HFH-11

Oxygen measurements in the control room were more likely to be representative, due to multiple sample points and the mixing effects of the fire plume jet.

rather poor. Finally, the control room visibility was well-predicted by the model, as may be seen in Figure 18.

4.2.2 Test HFH-12

Figures 19 - 26 make the same comparisons as Figures 11 - 18, except that data from test HFH-12 are used. In all cases, the model results for HFH-12 are essentially the same as those for HFH-11. This is to be expected, since the simulations differed only by a small change in the input HRR parameter. The comments made above, in reference to HFH-11, also apply to HFH-12. Corresponding test measurements showed a much larger difference between the HFH-11 and HFH-12, due to random variations in the test conditions.

5.0 CONCLUSIONS

We have developed a set of model inputs based, as closely as possible, on actual test conditions, and have shown that it is possible to use those inputs to simulate similar tests. In general, the correlation between the test results and the model predictions were very good. One interesting observation was that the air temperature predictions for spaces far from the fire compartment were typically better than those for the fire compartment itself. This is somewhat paradoxical, because one would expect that errors in the transport calculations would accumulate, leading to decreasing accuracy with increasing distance from the fire source. This may be due to the fact that the model predicts a single temperature for the entire space whereas the actual data corresponds to values at a finite number of discrete points. It is possible that the average of those point measurements did not reflect the true volume mean temperature. This discrepancy would likely be larger in spaces having greater temperature gradients, which would explain the trend in the deviations.

The observed lack of agreement between the torpedo room oxygen concentration and the model predictions is attributed to the number and positions of the gas sample points — in the torpedo room, there was only one and it was located low and forward of the fire. In that position, near the level of the bottom of the fire plume, the gas analyzers were likely responding primarily to the inflow of clean air from the safety door. This hypothesis is supported by the observation that the the measured oxygen concentration was approximately constant, at a value consistent with clean air, for the duration of the test.

In contrast, there were two sample points in the control room, one low and one high; the value shown in Figure 17 is the mean of the two. The primary mass transport from the torpedo room to the control room was via the framebay openings in the control room deck. The momentum provided by the vertical jets exiting from these ducts would be expected to cause very efficient mixing in the control room. Due to the combination of multiple sample points and good mixing, the control room measurements were more likely to be representative of the mean compartment concentrations than were the torpedo room values. These are special cases of the general principle that test data can be critically dependent on the locations of the instruments.

The weak correlation between soot yield and predicted air temperatures in the torpedo room (see Figure 5) suggests that FSSIM does not incorporate the effects of soot emission in the radiative

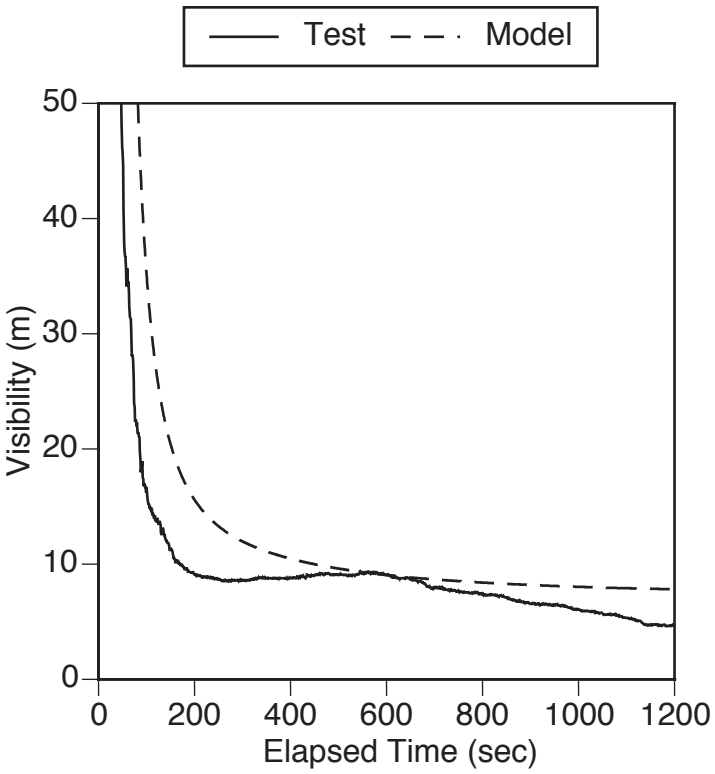

Figure 18. Control Room Visibility Comparison for HFH-11

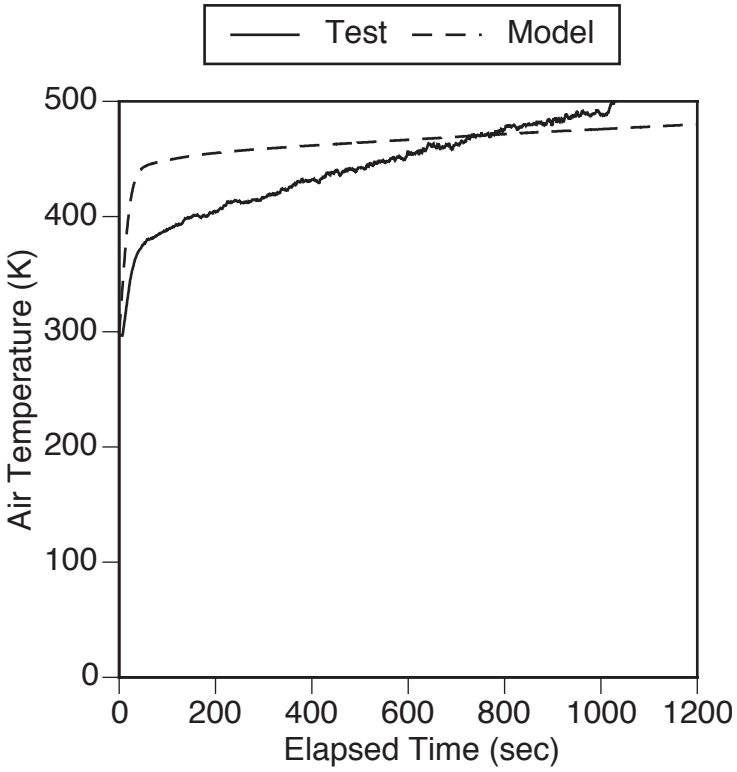

Figure 19. Torpedo Room Air Temperature Comparison for HFH-12

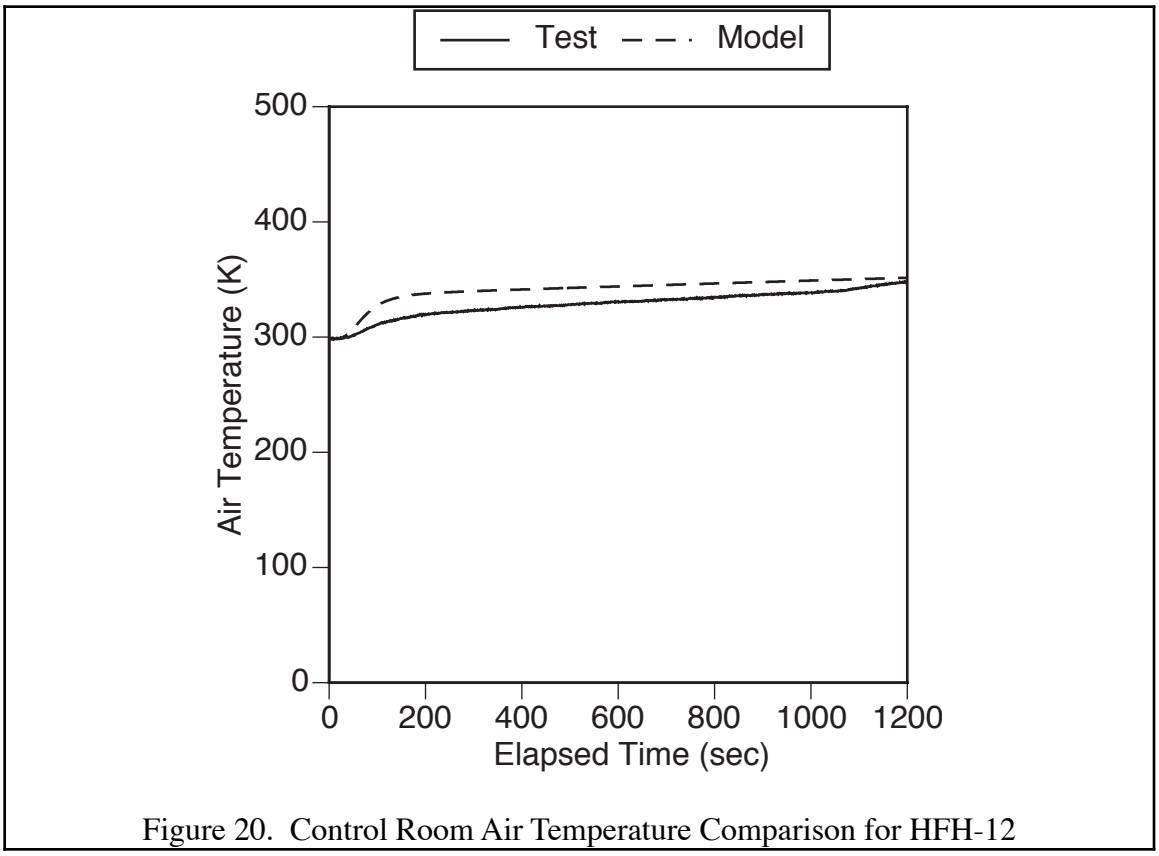

Figure 20. Control Room Air Temperature Comparison for HFH-12

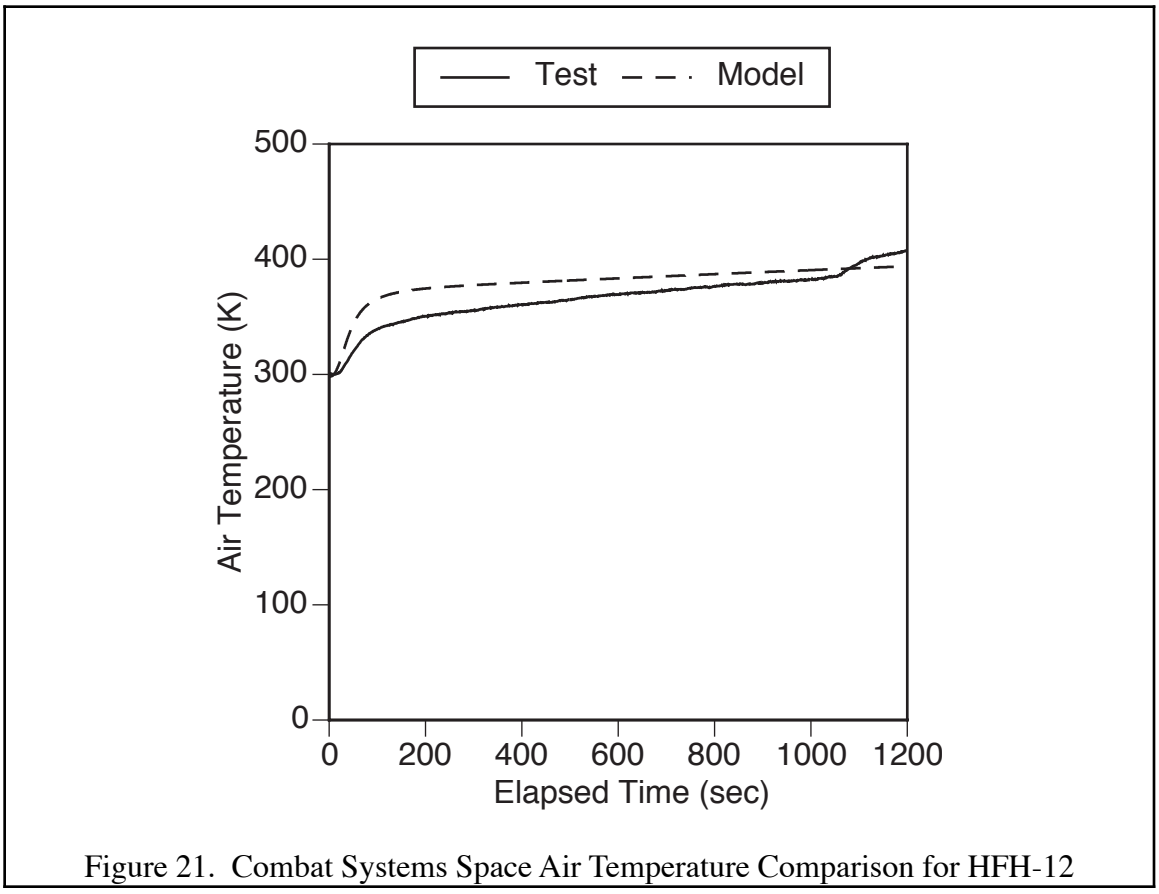

Figure 21. Combat Systems Space Air Temperature Comparison for HFH-12

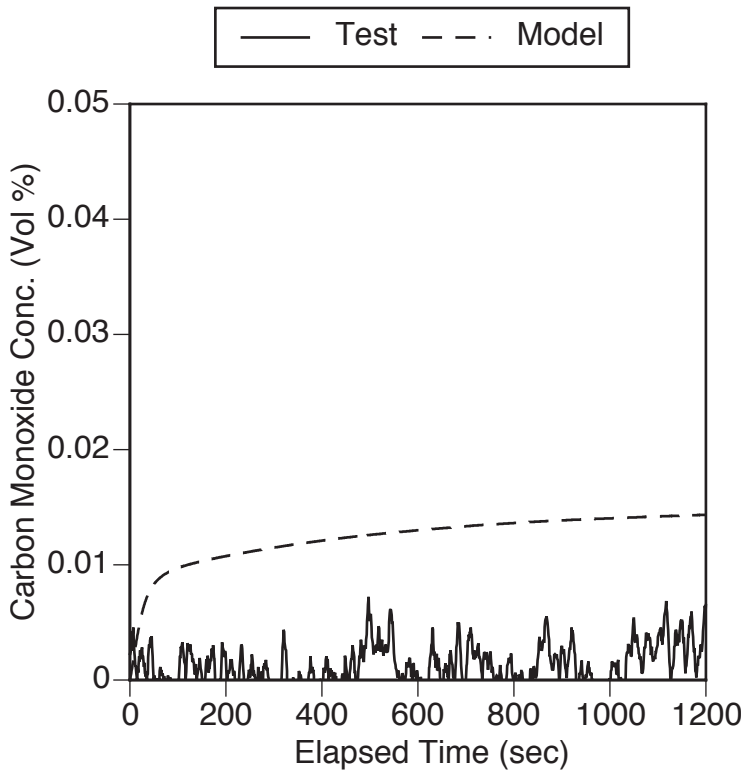

Figure 22. Torpedo Room Carbon Monoxide Comparison for HFH-12

Due to an instrument malfunction, no useful torpedo room carbon monoxide data were obtained for this test.

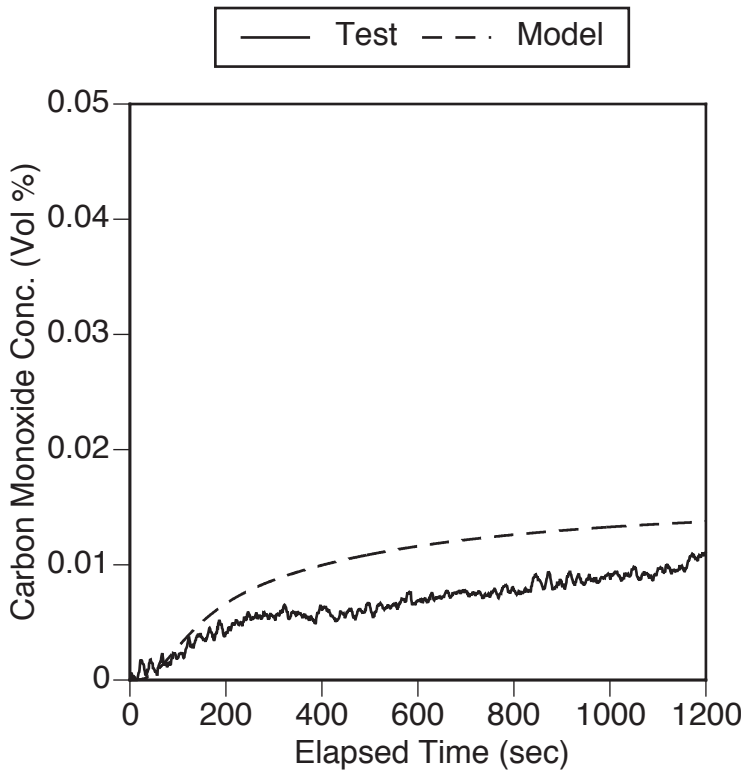

Figure 23. Control Room Carbon Monoxide Comparison for HFH-12

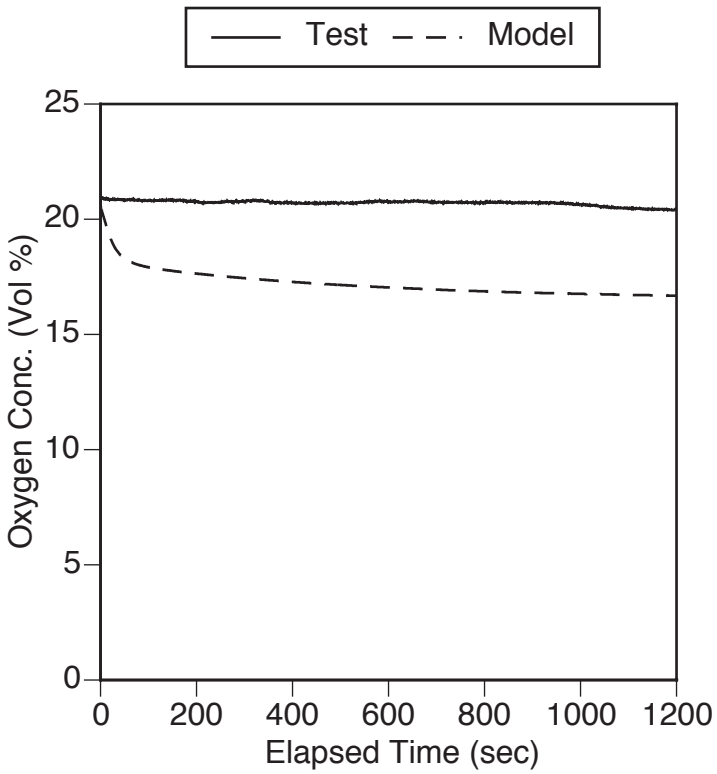

Figure 24. Torpedo Room Oxygen Comparison for HFH-12

Due to the location of the gas sampling point, the measured oxygen concentrations were not representative of the actual compartment average values in the torpedo room.

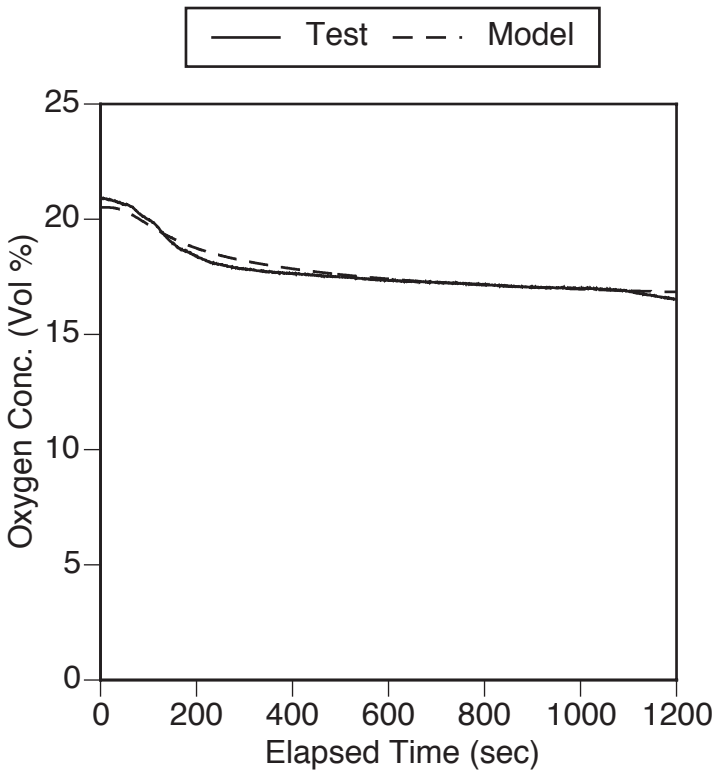

Figure 25. Control Room Oxygen Comparison for HFH-12

Oxygen measurements in the control room were more likely to be representative, due to multiple sample points and the mixing effects of the fire plume jet.

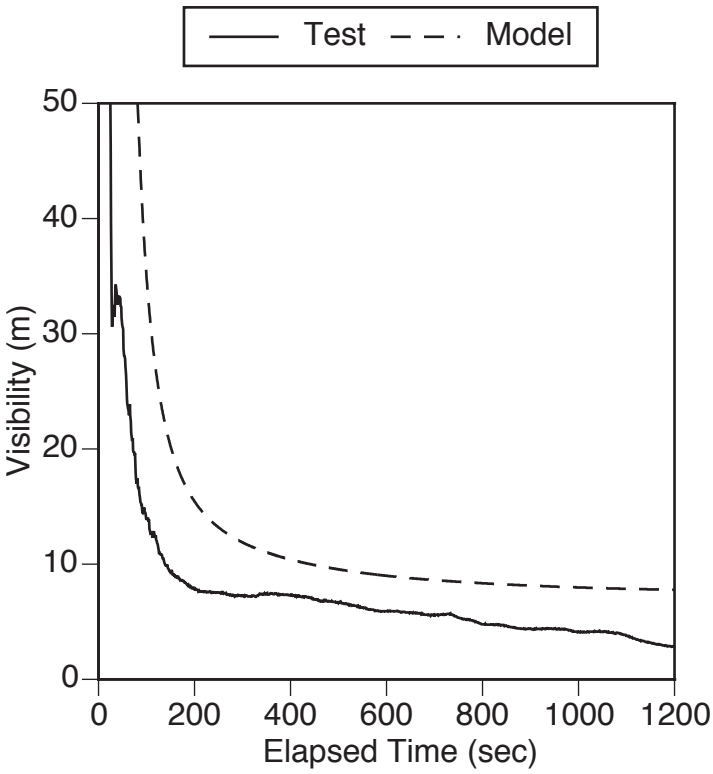

Figure 26. Control Room Visibility Comparison for HFH-12

transfer equations. Soot and carbon dioxide are both known to be significant contributors to radiation transfer [7] which, in turn, is a major controlling factor for both air and surface temperatures. This is an area in which FSSIM might benefit from additional development.

As was discussed above, under certain conditions the GUI counts the areas of open scuttles twice. At present, the work-around is to manually ensure that, when a hatch is open, the corresponding scuttle is closed. To simplify usage of the model, and reduce the chances of input errors, it would be advantageous to change the GUI so that this occurs automatically. This would require adding additional information to the database to associate specified pairs of hatches and scuttles.

6.0 REFERENCES

1. J.B. Hoover, C.L. Whitehurst, E.B. Chang and F.W. Williams, “Report of Fire Performance of Shipboard Electronic Space Materials,” NRL Letter Report 6180/0007, 12 January 2006.

2. J.B. Hoover, C.L. Whitehurst, E.B. Chang and F.W. Williams, “Final Report on Fire Performance of Shipboard Electronic Space Materials,” NRL Memo Report NRL/MR/6180--06-8983, 15 September 2006.

3. J.B. Hoover and F.W. Williams, “Test Plan: Fire Performance of Shipboard Dry Goods Storage Space Materials,” NRL Letter Report 6180/0172, 15 May 2006.

4. J.B. Hoover, H. Pham and F.W. Williams, “Heat Release Rates for Shipboard Dry Goods Storage Space Materials,” NRL Memo Report NRL/MR/6180--07-9045, 4 May 2007.

5. D. Halliday and R. Resnick,“Physics, Parts I and II,” Chapter 32, John Wiley & Sons, Inc., New York, 1966.

6. J.L. Bailey and P.A. Tatem, “Validation of Fire/Smoke Spread Model (CFAST) Using Ex-USS SHADWELL Internal Ship Conflagration Control (ISCC) Fire Tests,” NRL Memo Report NRL/MR/6180--95-7781, 30 September 1995.

7. J.B. Hoover, J.L. Bailey and P.A. Tatem, “An Improved Radiation Transport Submodel for CFAST,” *Combust. Sci. and Tech.*, 127, 213-229, 1997.

8. J.E. Floyd, S.P. Hunt, F.W. Williams and P.A. Tatem, “Fire and Smoke Simulator (FSSIM) Version 1 — Theory Manual,” NRL Memo Report NRL/MR/6180--04-8765, 31 March 2004.

9. J.E. Floyd, S.P. Hunt, P.A. Tatem and F.W. Williams, “Fire and Smoke Simulator (FSSIM) Version 1 – User’s Guide,” NRL Memo Report NRL/MR/6180--04-8806, 16 July 2004.

10. T.A. Haupt, D. Shulga, B. Sura, S.K. Durvasula, P.A. Tatem and F.W. Williams, “Simulation Environment for Onboard Fire Network Model Version 1.0 — Theory Manual,” NRL Memo Report NRL/MR/6180--04-8800, 12 May 2004.

11. T.A. Haupt, D. Shulga, B. Sura, S.K. Durvasula, P.A. Tatem and F.W. Williams, “Simulation Environment for Onboard Fire Network Model Version 1.0 — User’s Manual,” NRL Memo Report NRL/MR/6180--04-8801, 12 May 2004.

12. T.A. Haupt, G. Henley, B. Sura, R. Kirkland, J. Floyd, J. Scheffey, P.A. Tatem and F.W. Williams, “User Manual for Graphical User Interface Version 2.4 with Fire and Smoke Simulation Model (FSSIM) Version 1.2,” NRL Memo Report NRL/MR/6180--06-9013, 18 December 2006.

13. J.B. Hoover, J.L. Bailey, H.D. Willauer and F.W. Williams, “Submarine Hydraulic Fluid Explosion Mitigation and Fire Threats to Ordnance,” NRL Memorandum Report NRL/MR/6180--05-8859, 18 January 2005.

14. J.B. Hoover, J.L. Bailey, H.D. Willauer and F.W. Williams, “Evaluation of Submarine Hydraulic System Explosion and Fire Hazards,” NRL Memorandum Report NRL/MR/6180--05-8908, 29 September 2005.

15. Commander Naval Sea Systems Command, SEA 05Q, “Performance Specification, Lubricating Oil, Steam Turbine and Gear, Moderate Service,” Military Specification MIL-PRF-17331J, 09 September 2003 (Superseding MIL-PRF-17331H (SH).

16. R. Moore, personal communication, Bete Fog Nozzles, Greenfield, MA, 28 January 2004.

17. G.W. Mulholland, “Smoke Production and Properties,” in SFPE Handbook of Fire Protection Engineering, 1st Ed., National Fire Protection Association, Quincy, MA, p.1-373, 1988.

18. J.B. Hoover and P.A. Tatem, “Application of CFAST to Shipboard Fire Modeling I. Development of the Fire Specification,” NRL Memorandum Report NRL/MR/6180--00-8466, 29 June 2000.

ACKNOWLEDGMENTS

This work would not have been possible without the hard work of the men and women assigned to the ex-USS SHADWELL facility. We would especially like to thank Robert Burgess, Vonnie Byrd, Matt Harrison, Carl Krueger, Xuanan Nguyen, Josh Odem, Hung Pham, Russell Robertson, Manton Smith and the many students who prepared the test area, installed the instruments and helped conduct the tests.

Finally, our thanks to the safety officers, Chelbi Cole and John Farley, and to Brad Havlovick and the personnel of Havlovick Engineering Services for their support.

APPENDIX A. INSTRUMENTATION LOCATIONS

This Appendix includes drawings showing the instrument layouts for the critical compartments discussed in this report. Instrument types are given by the symbols shown in the legend.

CONTENTS

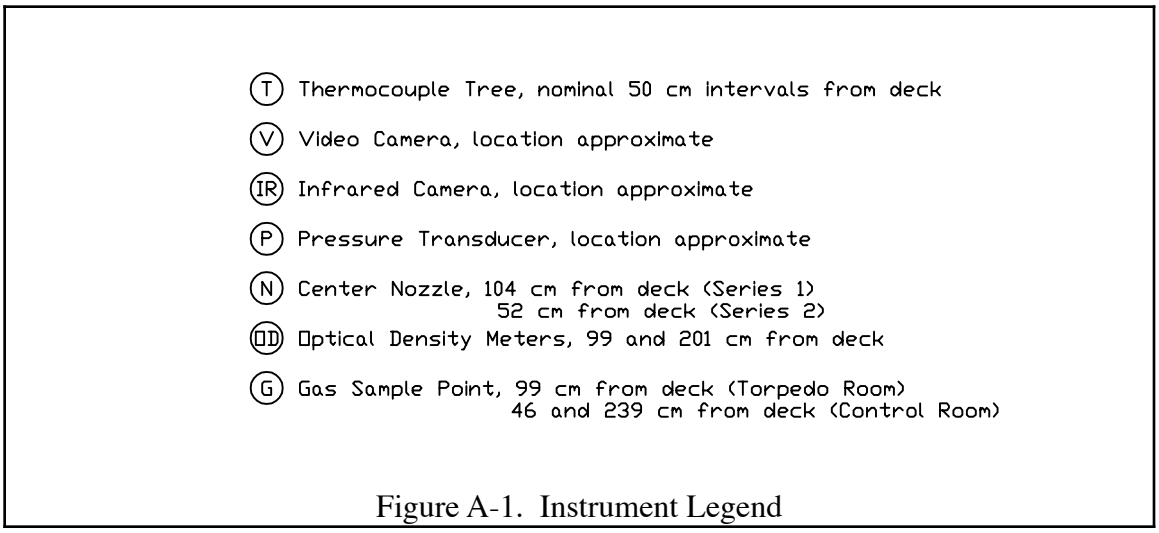

Figure A-1. Instrument Legend

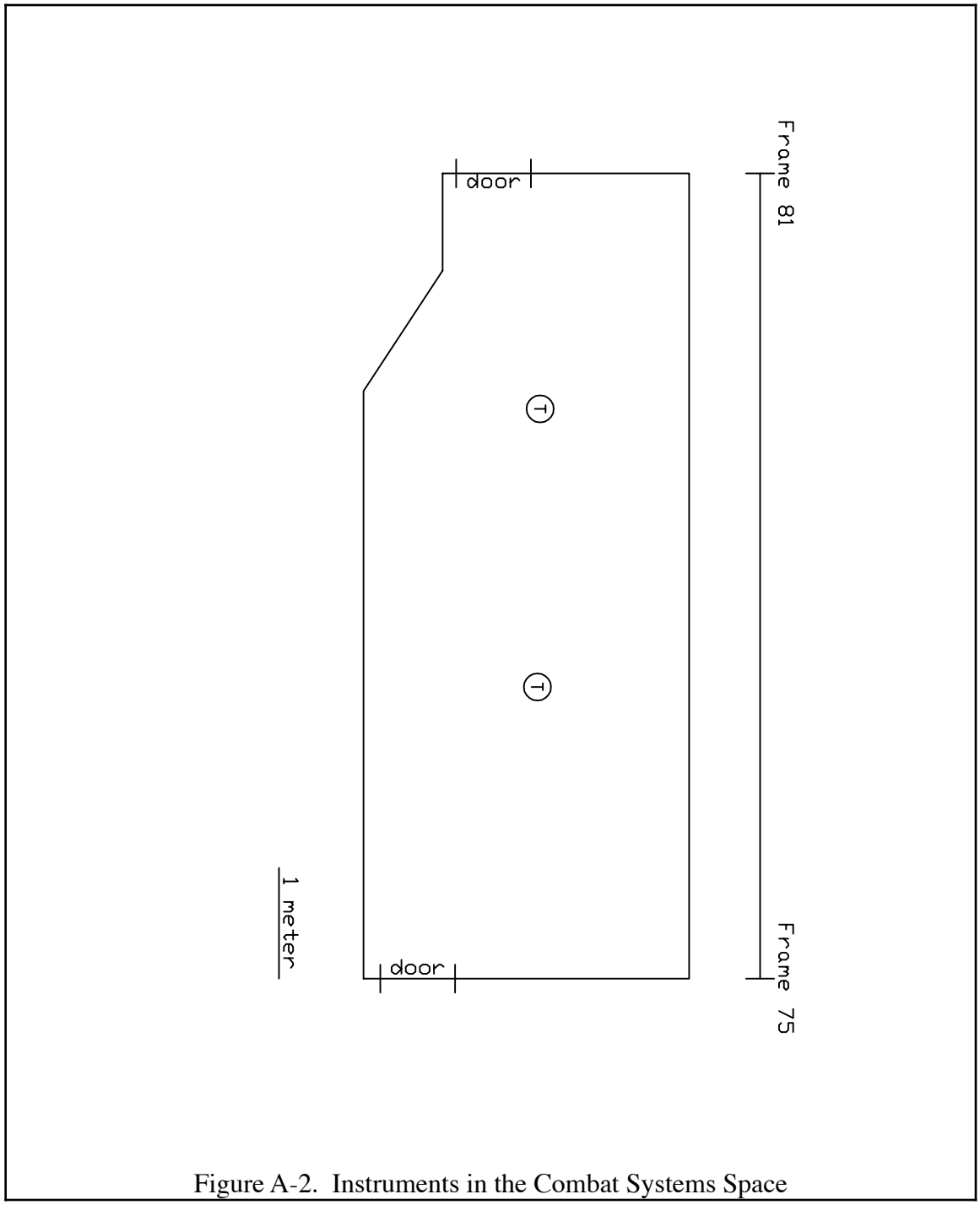

Figure A-2. Instruments in the Combat Systems Space

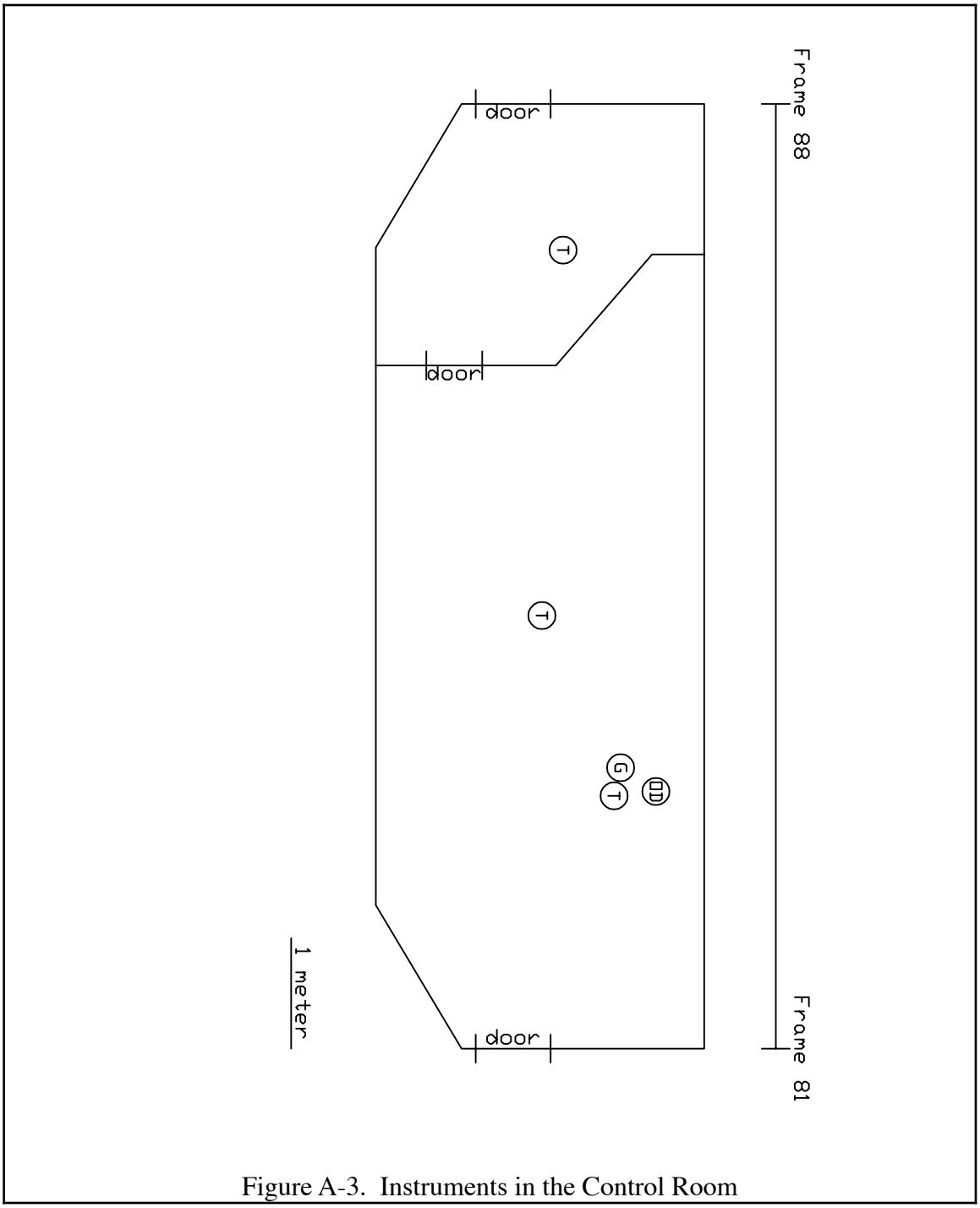

Figure A-3. Instruments in the Control Room

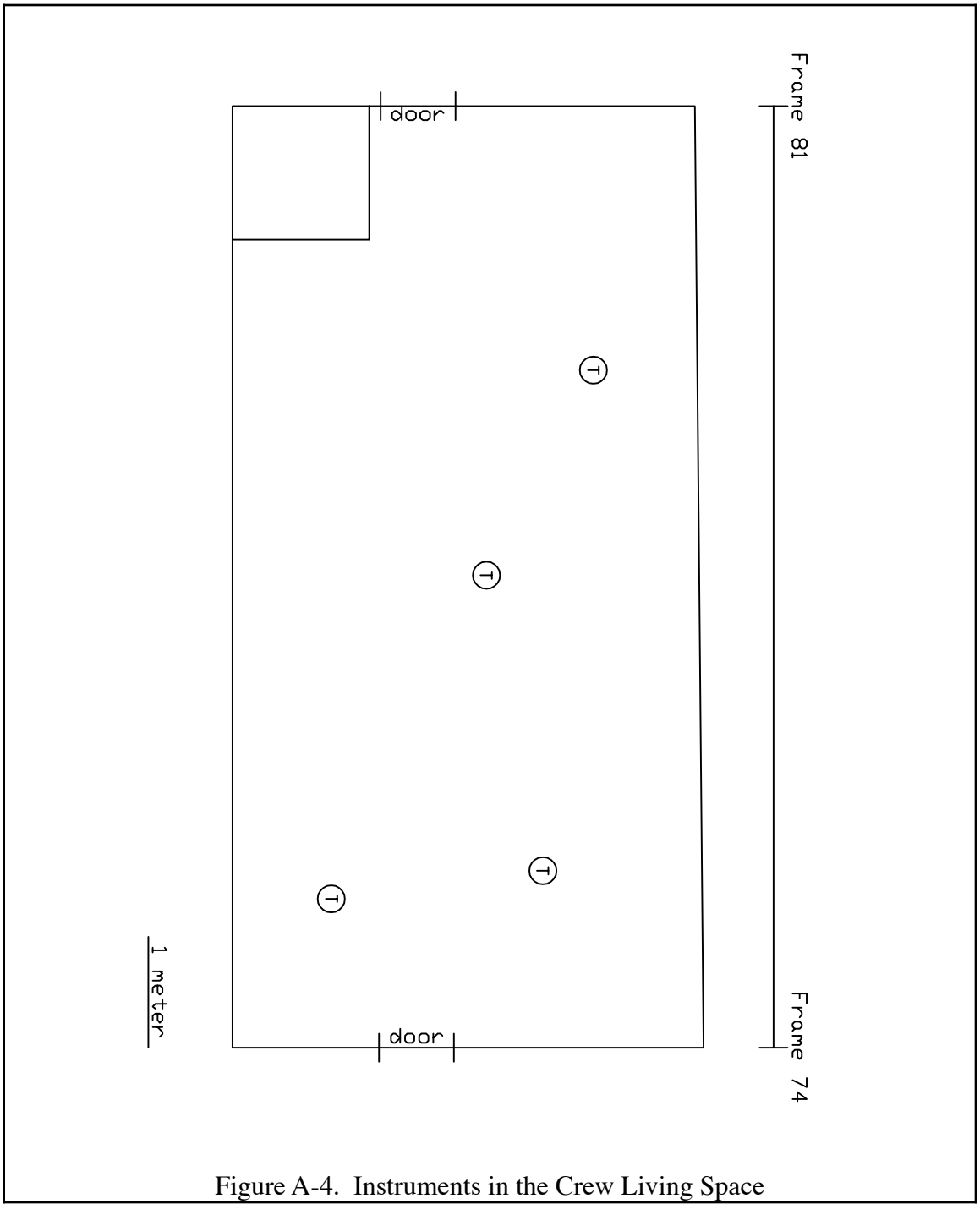

Figure A-4. Instruments in the Crew Living Space

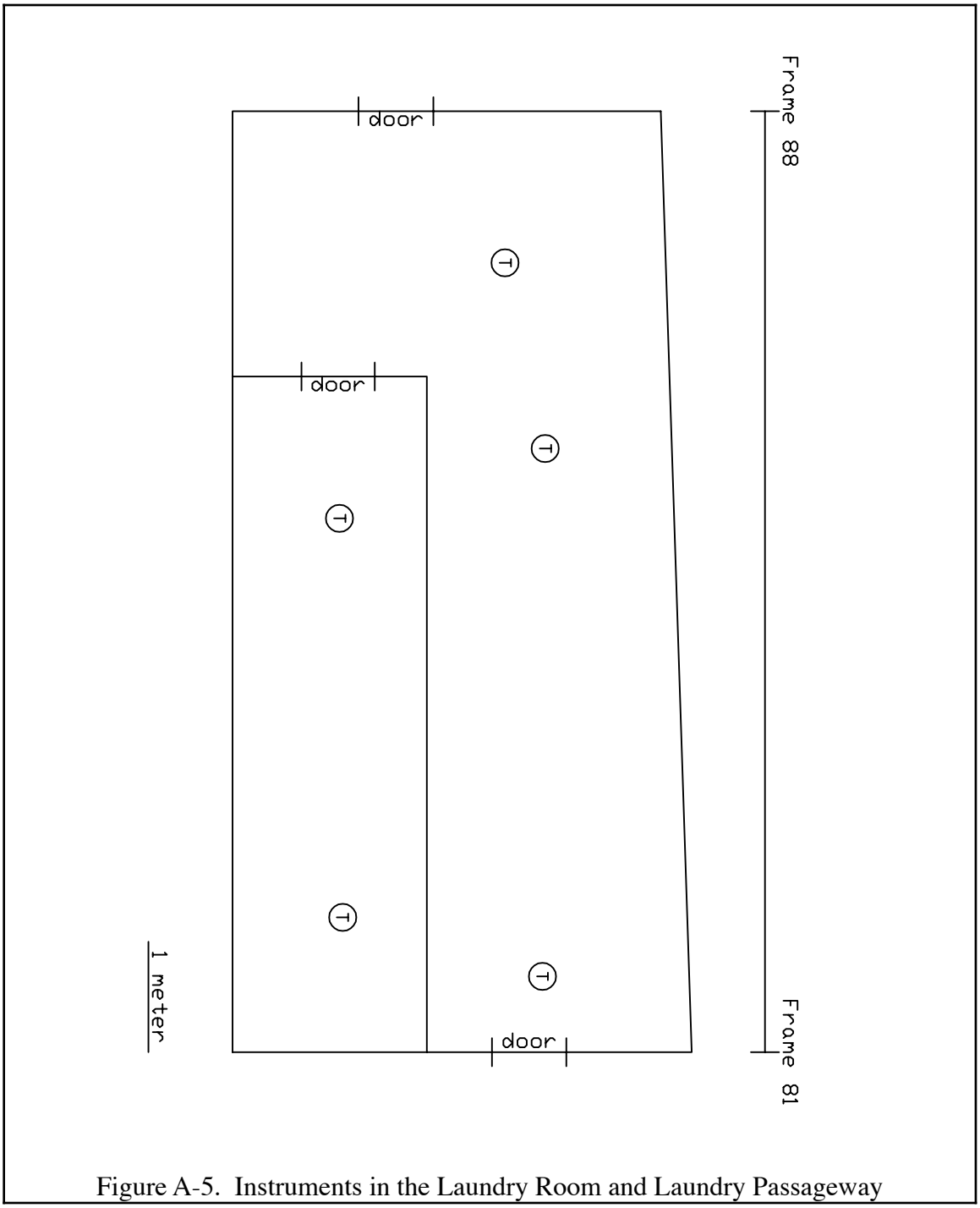

Figure A-5. Instruments in the Laundry Room and Laundry Passageway

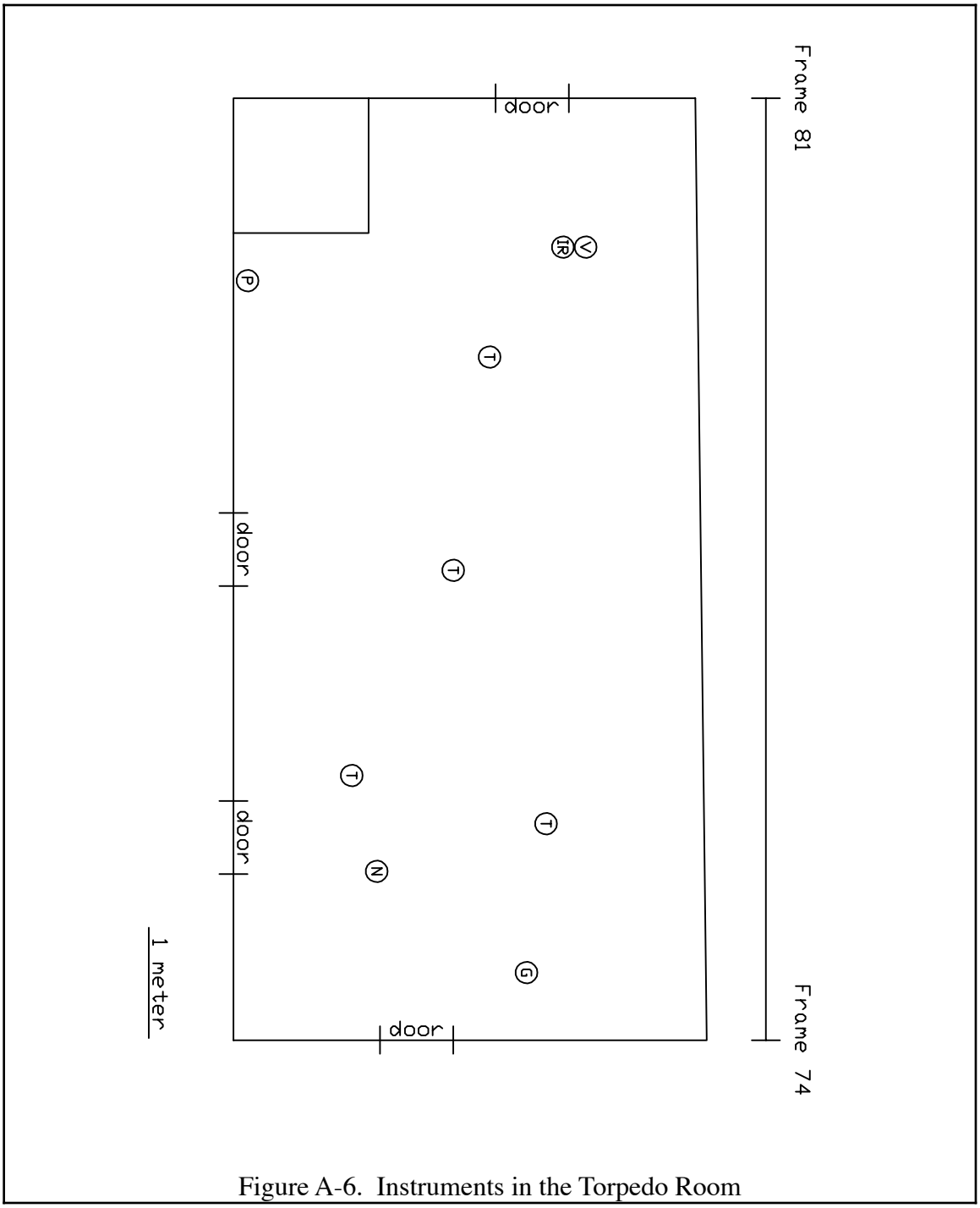

Figure A-6. Instruments in the Torpedo Room

APPENDIX B. HFH-11 RESULTS

This Appendix compares the test and simulation results for the HFH-11 submarine hydraulic fire hazard test.

CONTENTS

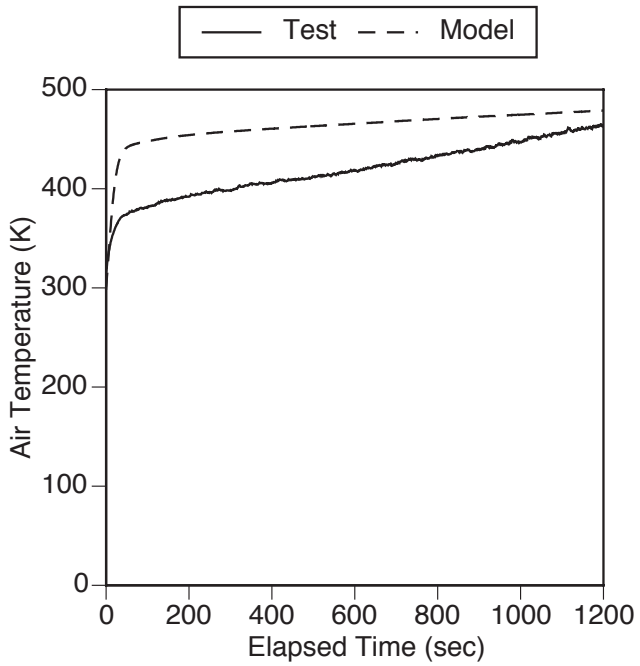

Figure B-1. Torpedo Room Air Temperature

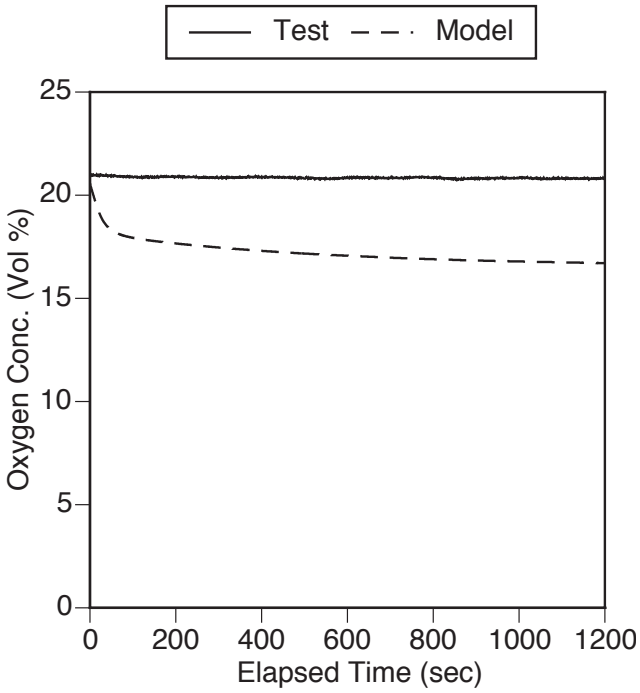

Figure B-2. Torpedo Room Oxygen Concentration

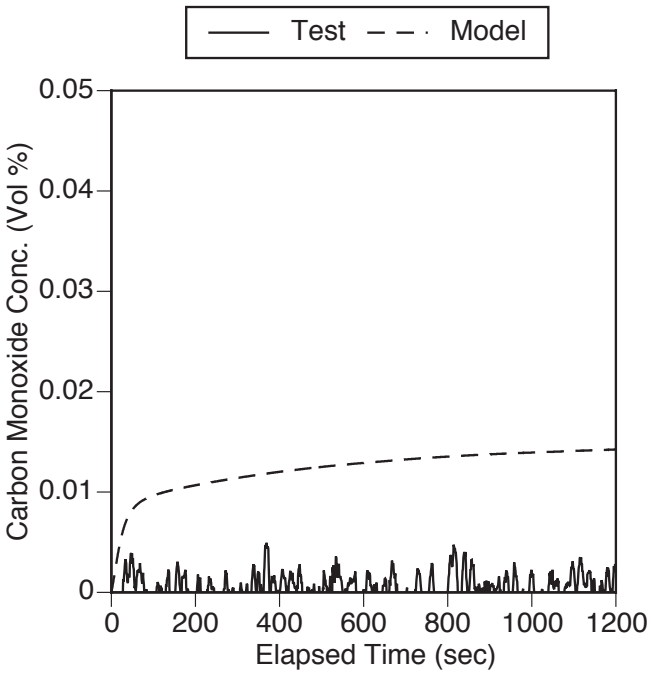

Figure B-3. Torpedo Room Carbon Monoxide Concentration

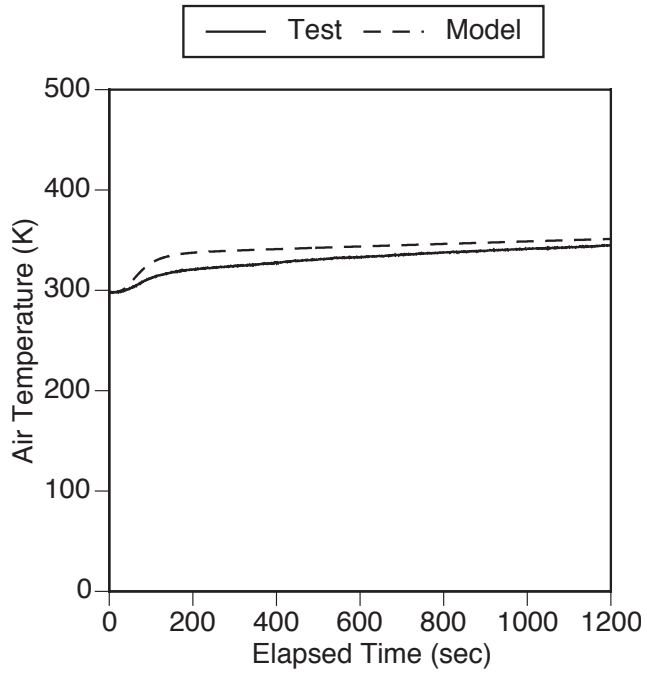

Figure B-4. Control Room Air Temperature

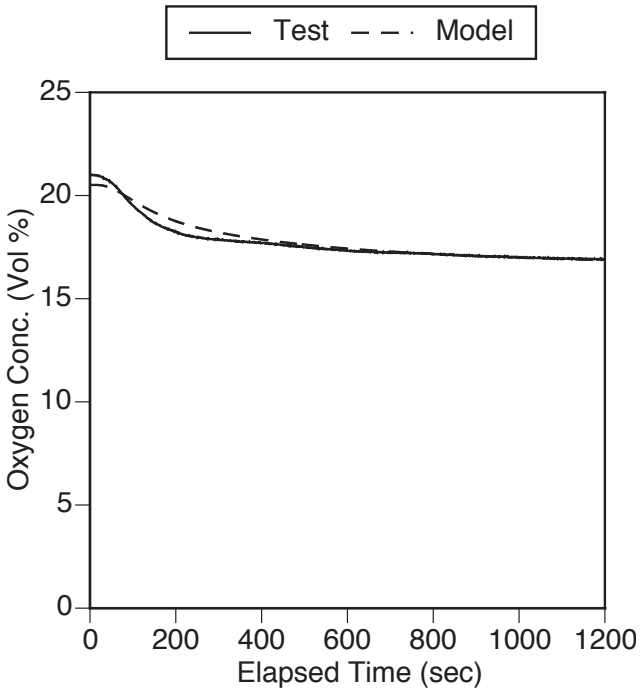

Figure B-4. Control Room Oxygen Concentration

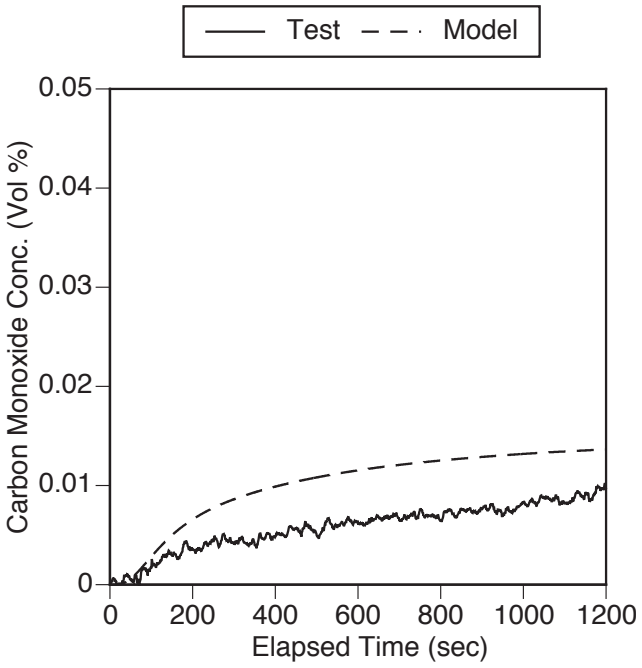

Figure B-6. Control Room Carbon Monoxide Concentration

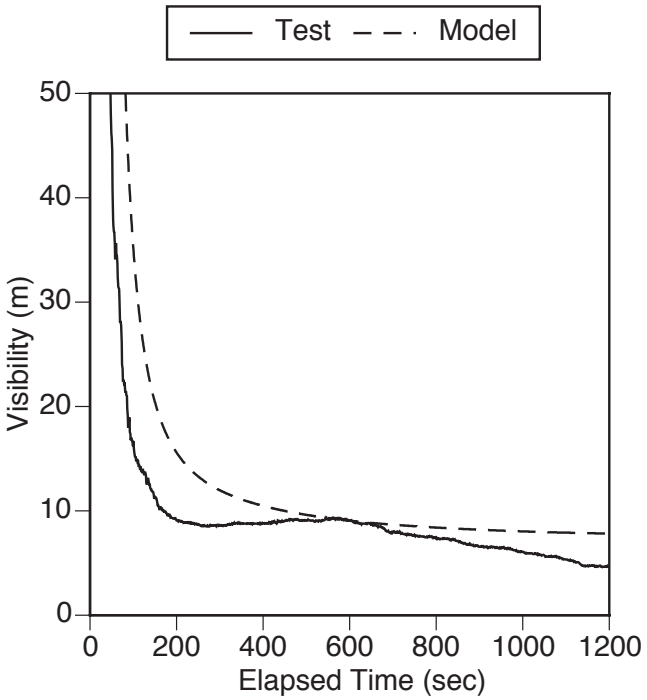

Figure B-7. Control Room Visibility

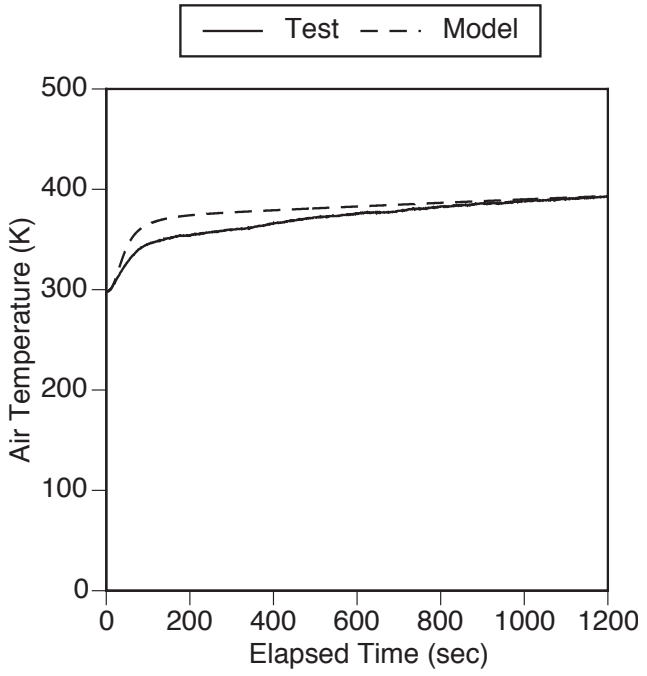

Figure B-8. Combat Systems Space Air Temperature

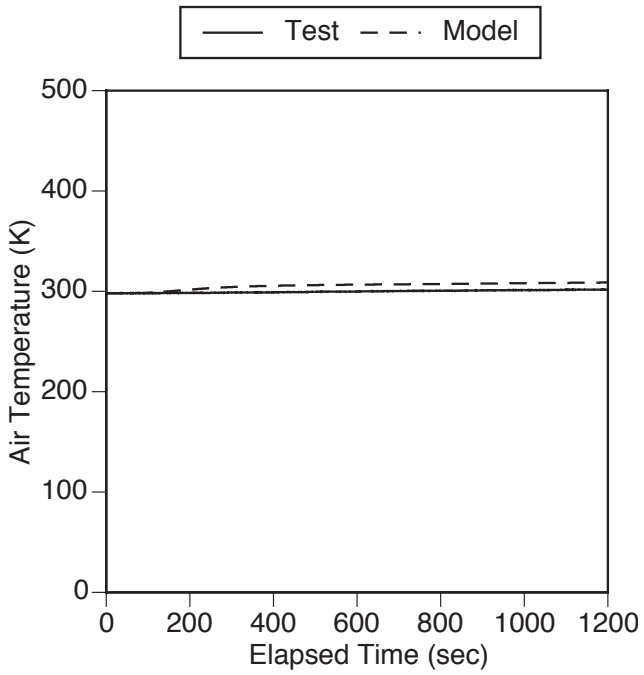

Figure B-9. Crew/CPO Mess Air Temperature

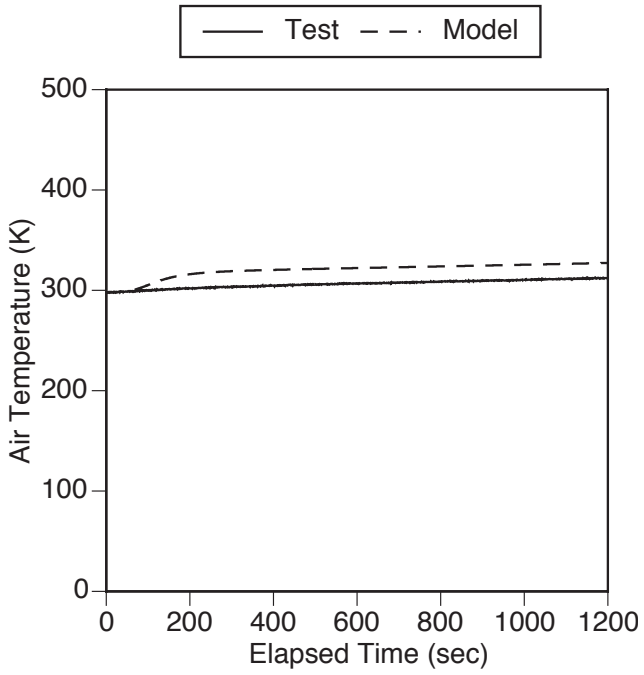

Figure B-10. Wardroom Air Temperature

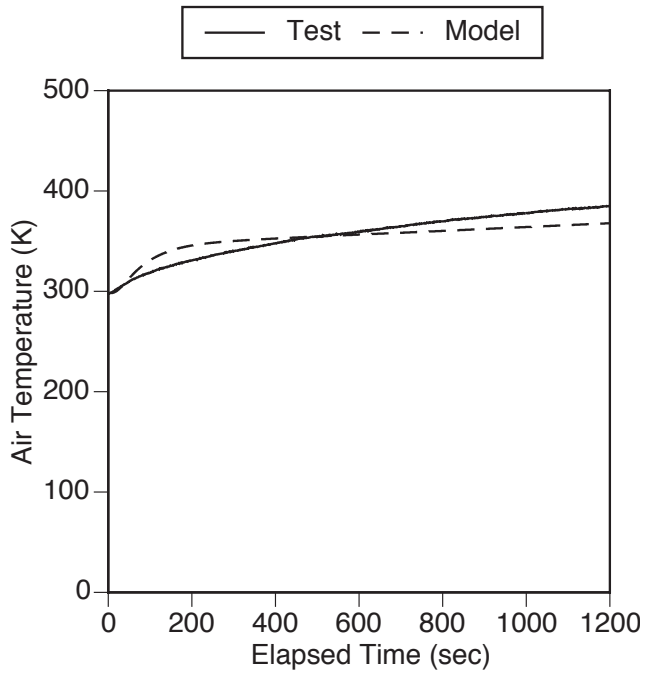

Figure B-11. Crew Living Air Temperature

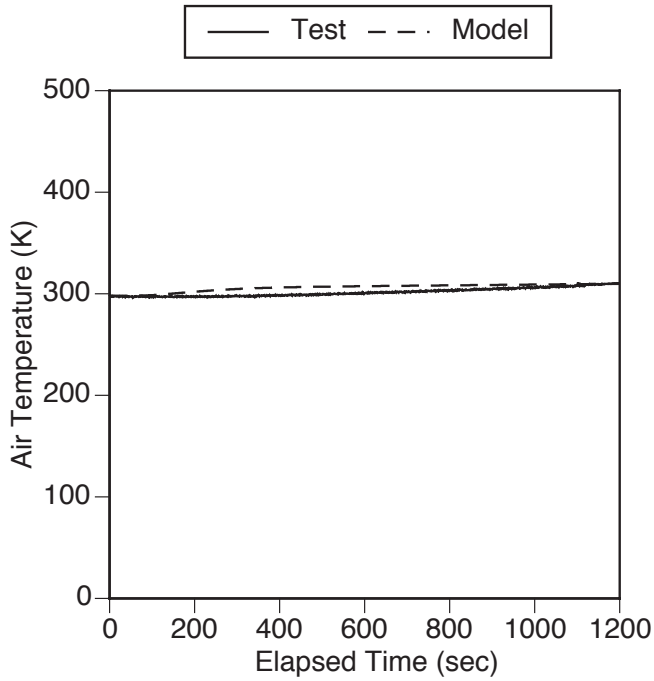

Figure B-12. AMR Air Temperature

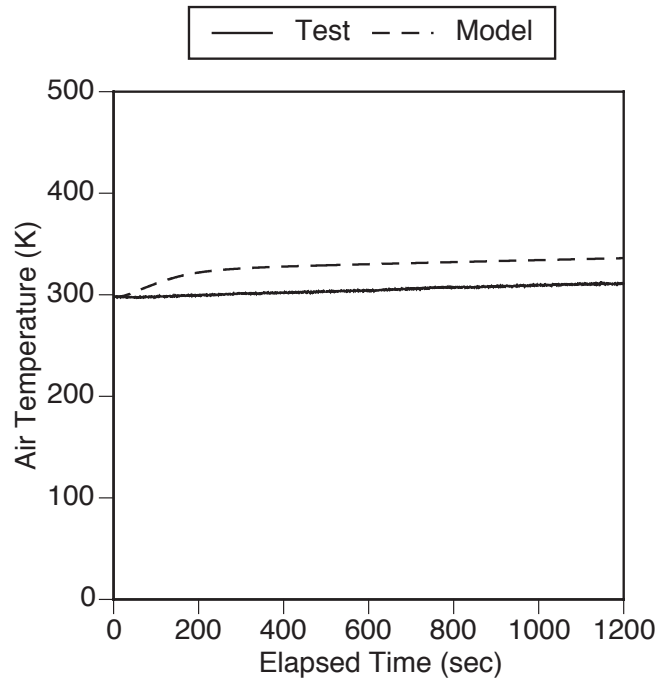

Figure B-13. Laundry Room Passageway Air Temperature

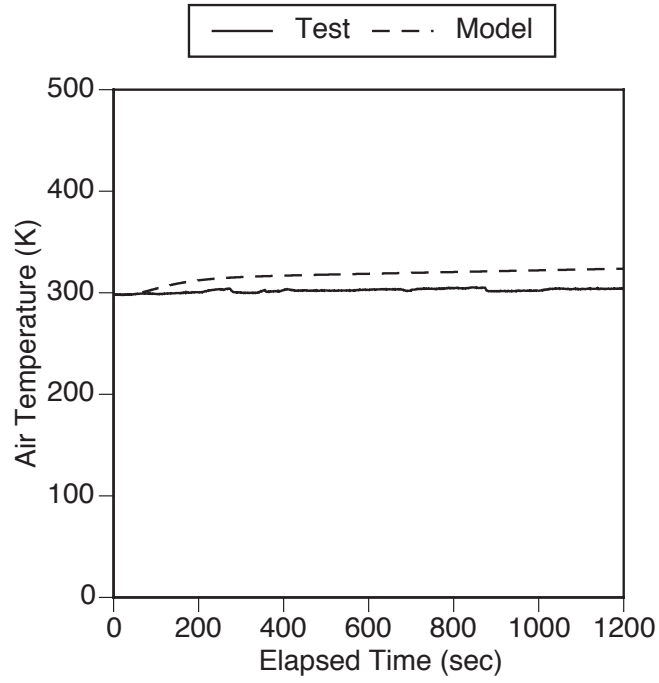

Figure B-14. Laundry Room Air Temperature

APPENDIX C. HFH-12 RESULTS

This Appendix compares the test and simulation results for the HFH-12 submarine hydraulic fire hazard test.

CONTENTS

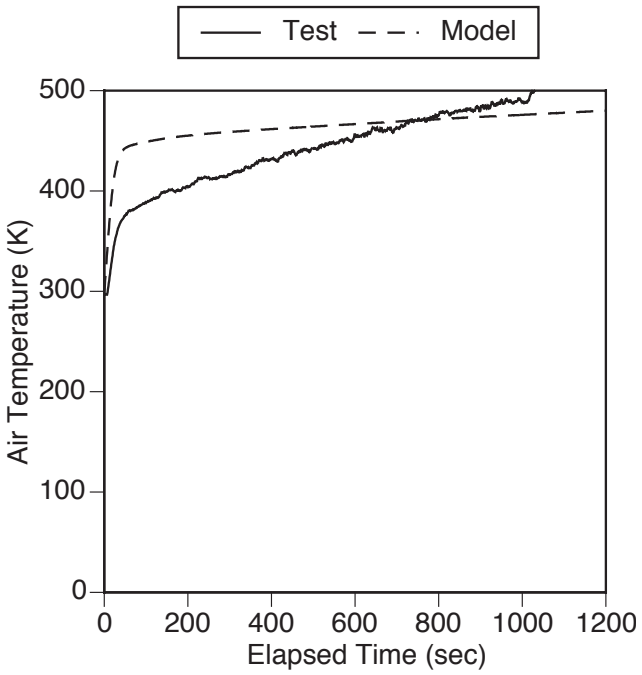

Figure C-1. Torpedo Room Air Temperature

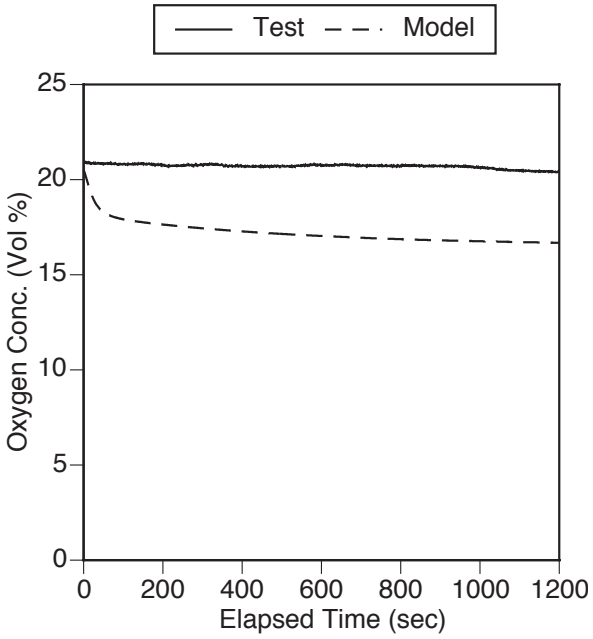

Figure C-2. Torpedo Room Oxygen

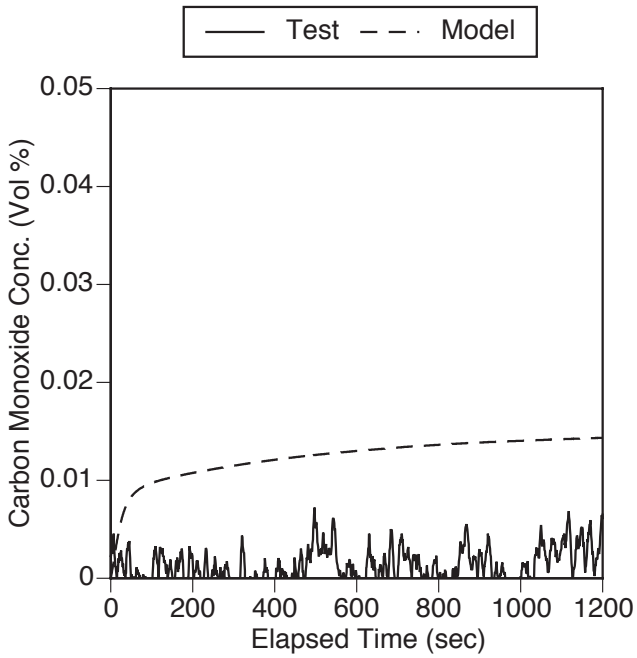

Figure C-3. Torpedo Room Carbon Monoxide

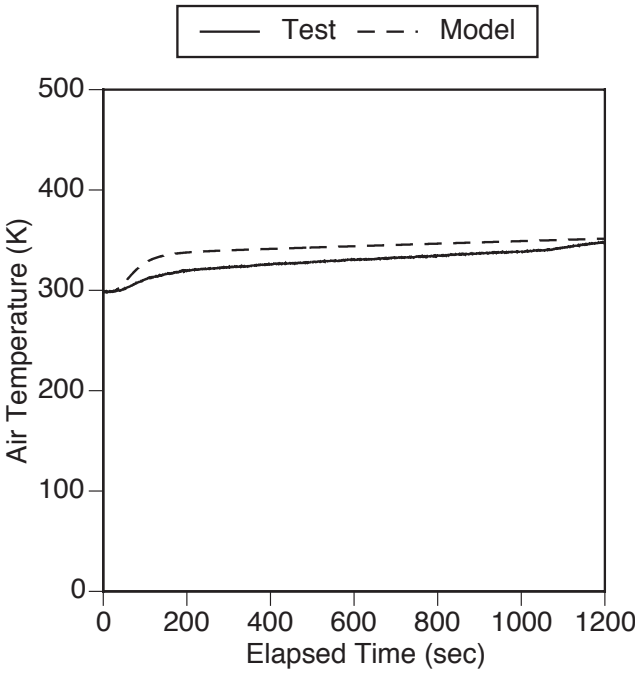

Figure C-4. Control Room Air Temperature

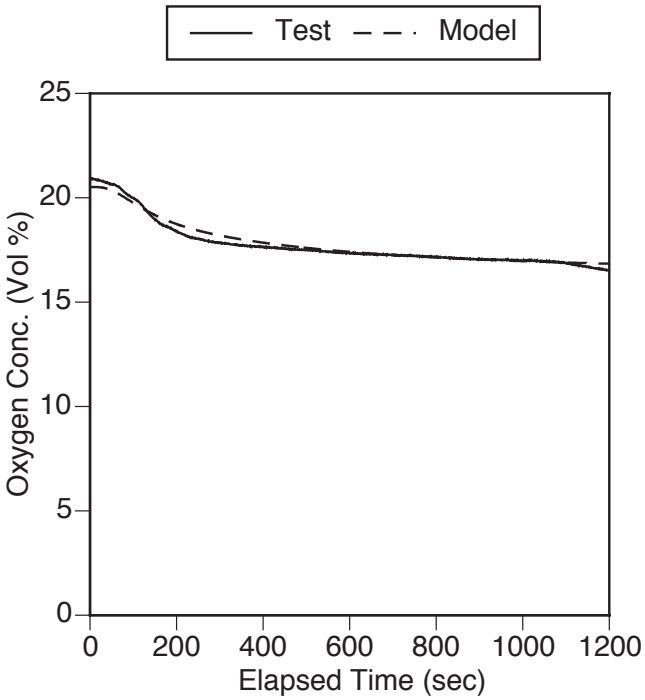

Figure C-5. Control Room Oxygen

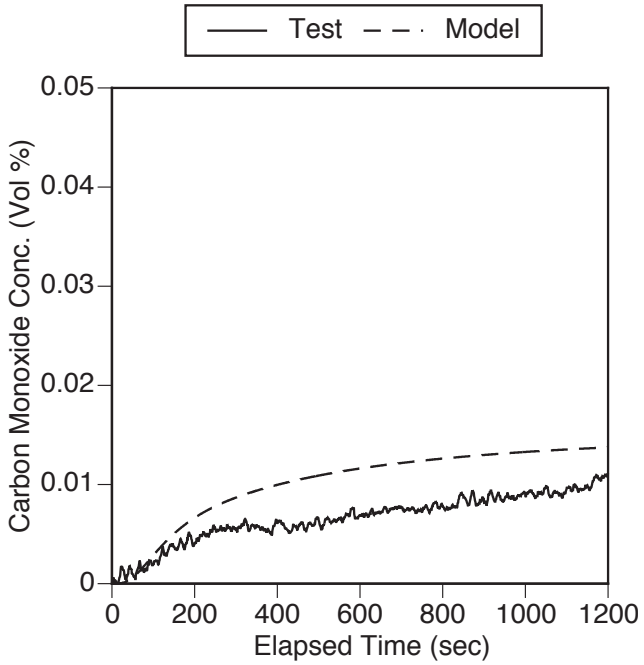

Figure C-6. Control Room Carbon Monoxide

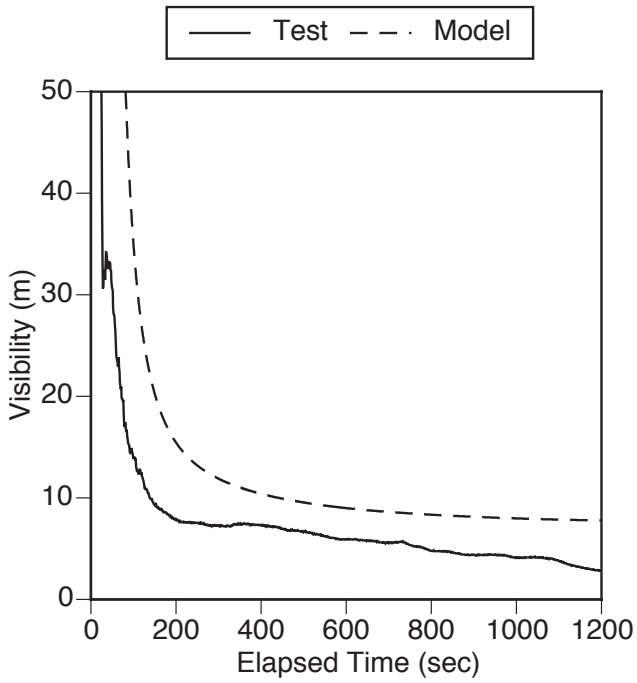

Figure C-7. Control Room Visibility

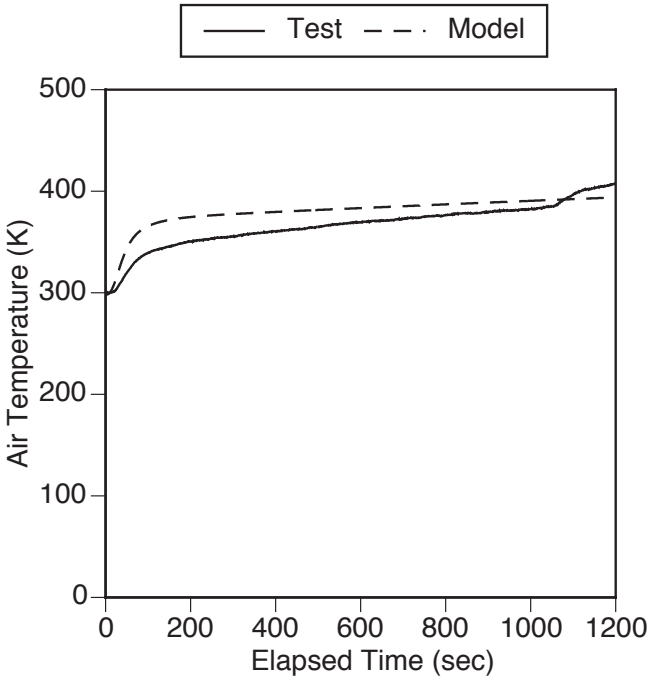

Figure C-8. Combat Systems Space Air Temperature

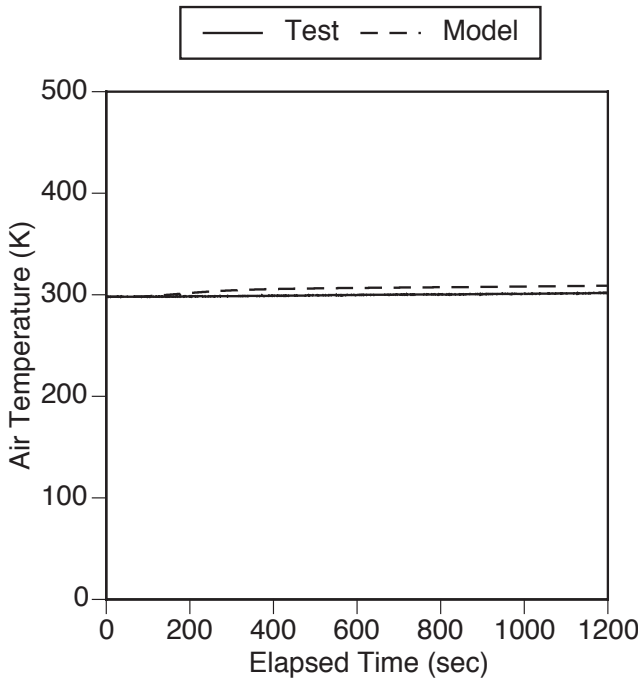

Figure C-9. Crew/CPO Mess Air Temperature

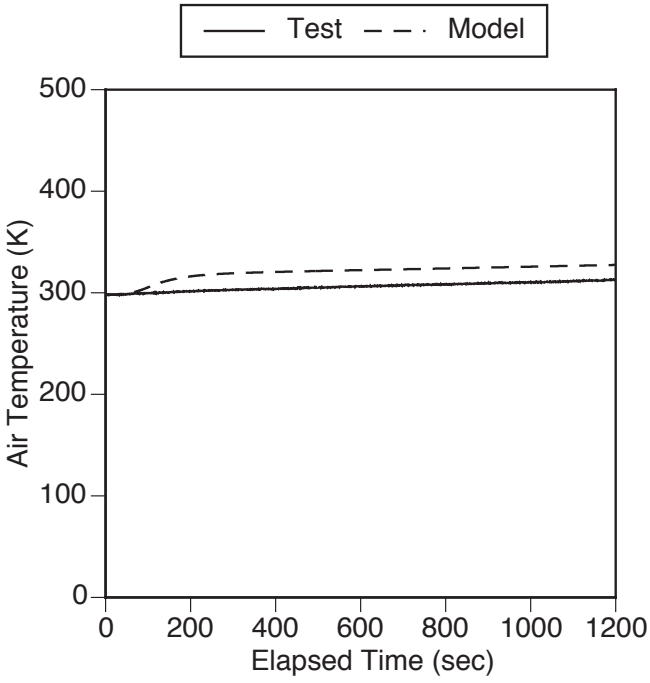

Figure C-10. Wardroom Air Temperature

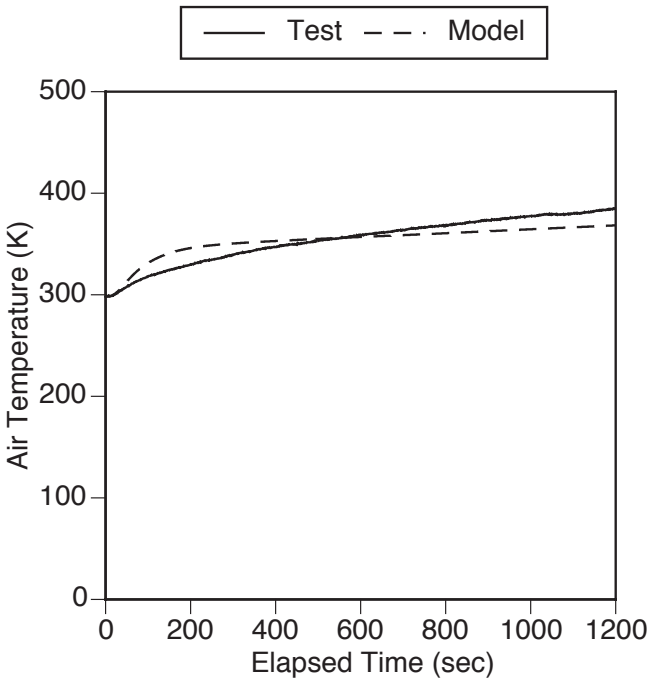

Figure C-11. Crew Living Air Temperature

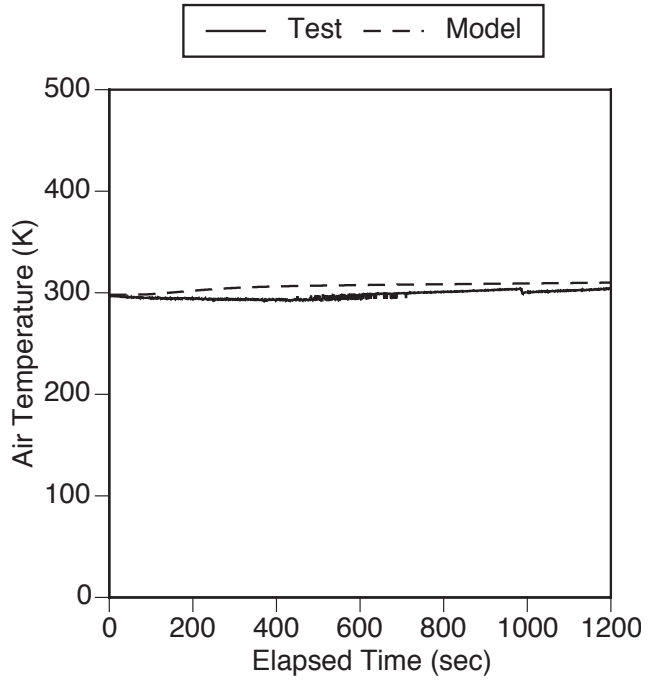

Figure C-12. AMR Air Temperature

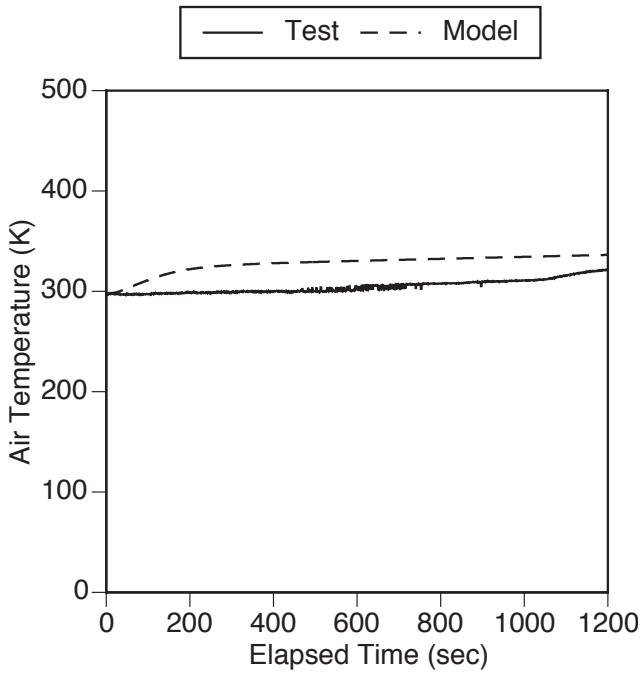

Figure C-13. Laundry Room Passageway Air Temperature

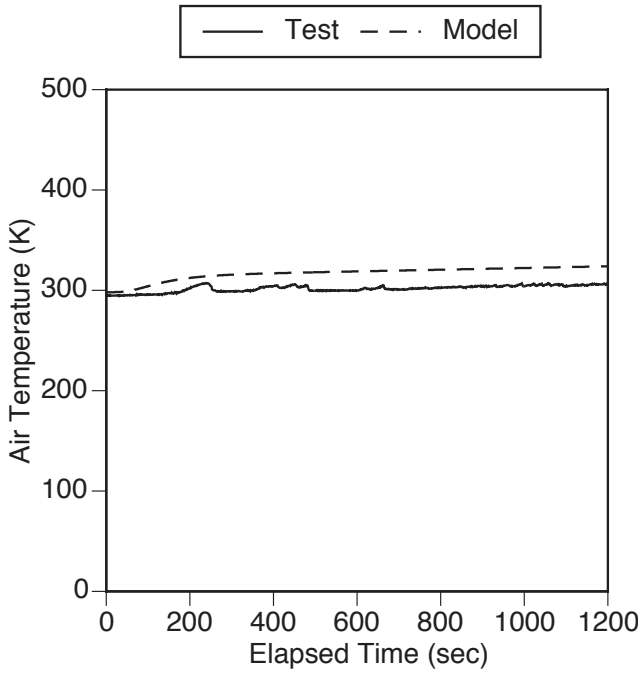

Figure C-14. Laundry Room Air Temperature